UNIVERSITÀ
DEGLI STUDI
DI TRIESTE

UNIVERSITÀ DEGLI STUDI DI TRIESTE

XXXIV CICLO DEL DOTTORATO DI RICERCA IN

SCIENZE DELLA RIPRODUZIONE E DELLO SVILUPPO

DEVELOPMENT AND CHARACTERIZATION OF POLYSACCHARIDE-BASED SCAFFOLDS WITH ANTIMICROBIAL FEATURES FOR TISSUE REGENERATION

Settore scientifico-disciplinare: MED/50 Scienze Tecniche Mediche Applicate

DOTTORANDO
MARIO MARDIROSSIAN

COORDINATORE
PROF. PAOLO GASPARINI

SUPERVISORE DI TESI
PROF. GIANLUCA TURCO

CO-SUPERVISORE DI TESI
DAVIDE PORRELLI

ANNO ACCADEMICO 2020/2021

TABLE OF CONTENTS

ABSTRACT

Bone defects represent a still unsolved clinical problem that needs the attention of biomedical research. With the aim to promote the bone regeneration of orthopaedic defects, medicine refers to tissue engineering, which invests significant efforts in developing scaffolds to assist the healing of the injured tissues. Porous three-dimensional scaffolds are very efficient in helping the regeneration of damaged bone, and within the galaxy of different types of scaffolds, those composed of alginate and hydroxyapatite are well characterized and quoted. However, even the most efficient scaffold would be useless in case of infection in its grafting site. In order to develop scaffolds with suitable chances to effectively address the problem of bone regeneration, those structures should therefore be endowed also with antimicrobial properties. Any anti-infective feature of scaffolds however should never be designed at expense of the biocompatibility of these structures and of their capability to promote tissue regeneration. Furthermore, looking for the development of long-term scaffolds to be exploited in the upcoming future, it is becoming more and more clear that these structures shall not rely on ordinary antibiotics for their antimicrobial features. We are in fact entering the so-called post-antibiotic age due to bacterial antibiotic resistance, that is making useless most of the antibiotics that are currently used in clinic. The need for new antimicrobials is therefore evident, and in this scenario, the antimicrobial peptides (AMPs) are receiving increasing attention because of their antibacterial properties. Among AMPs, the proline-rich AMPs (PrAMPs) are particularly interesting because they combine the antimicrobial potency of AMPs with reassuring biocompatibility, avoiding cytotoxicity issues that affect several other AMPs classes.

Aim of this project was to load a rationally optimized PrAMP on alginate/hydroxyapatite (Alg/HAp) scaffolds to provide antimicrobial matrices retaining the capability of Alg/HAp scaffolds to assist bone regeneration.

As first, in order to tailor PrAMPs antimicrobial activity to better target orthopaedic surgical pathogens, the PrAMP Bac7(1-16) was modified by replacing some aminoacidic residues. Subsequently, a lipid moiety was also added to the N-terminus of the modified peptide. Only the first approach was successful providing the B7-005, a new PrAMP displaying broader and more efficient antimicrobial activity. On the other hand, the lipidation of B7-005 was detrimental, since it did not improve the antimicrobial properties of the peptide but worsened markedly its biocompatibility toward human cells.

Then, according to a well characterized protocol, Alg/HAp scaffolds were produced and, after preparatory setting, efficiently loaded with B7-005 by surface adsorption. However, once adsorbed on the scaffold, the peptide was firmly retained on the structure, and could not be released in solution due to the strong electrostatic interaction occurring between alginate and B7-005. The attempts to modulate the electrostatic interaction, by reducing the surface charge of the scaffolds using a lactose-modified chitosan, were useless. Alginate-based structures therefore turned out to be scarcely compatible with cationic AMPs.

In order to prepare scaffolds compatible with the loading and release of B7-005, a protocol to substitute the alginate with agarose during the scaffold preparation was set up. Agarose/Hydroxyapatite (Aga/HAp) porous three-dimensional scaffolds were prepared maintaining the proportion between polysaccharide and ceramic previously used for the Alg/HAp system. SEM imaging and microcomputed tomography indicated that Aga/HAp scaffolds displayed overall porosity, as well as pores dimension and interconnection were similar to Alg/HAp scaffold. Aga/HAp scaffolds were then considered suitable for bone-regeneration purposes.

The newly developed Aga/HAp scaffolds were loaded with B7-005 by freeze-drying, and they displayed a subsequent effective release of peptide. A human bony cell line was used for biocompatibility assay, indicating that Alg/HAp scaffolds are compatible with human cells, that could adhere and proliferate on them. Moreover, it has been then shown that cells can proliferate also on scaffolds treated with B7-005, although their proliferation rate was reduced in the first period.

Aga/HAp scaffolds were further analysed and displayed swelling behaviour limited to very short timings. The porous structures displayed basically very low mechanical resistance during compression tests, but on the other hand their stability was constant over time, showing no signs of degradation after incubation in simulated body fluids up to 2 months.

As last, it has been shown that B7-005 Aga/HAp scaffolds can inhibit the growth of bacterial pathogens of clinical relevance, although there is still space for optimization to improve their antimicrobial properties.

Taken together, results collected in the present work demonstrated that agarose is more suitable than alginate for the combined use of polysaccharide and cationic antimicrobial peptides. It has moreover been shown that it is possible to replace alginate with agarose in a protocol to produce three-dimensional porous scaffolds, maintaining several desirable properties of the well characterized Alg/HAp scaffolds.

RIASSUNTO

I difetti ossei rappresentano un problema clinico tuttora irrisolto che necessita dell'attenzione della ricerca biomedica. Per promuovere la rigenerazione ossea in caso di difetti ortopedici, la medicina si rivolge all'ingegneria tessutale, la quale investe notevoli sforzi nello sviluppo di scaffold per aiutare la guarigione di tessuti lesionati. Gli scaffold porosi tridimensionali sono molto efficienti nell'aiutare la rigenerazione dell'osso danneggiato, e nella galassia dei diversi tipi di scaffold, quelli composti di alginato ed idrossiapatite sono ben caratterizzati e quotati. Tuttavia, persino lo scaffold più efficiente sarebbe inutile in caso di infezione del sito di impianto. Per sviluppare scaffold con effettive possibilità di risolvere in modo efficace il problema della rigenerazione ossea, tali strutture dovrebbero possedere anche proprietà antimicrobiche. Ad ogni modo, quale che sia l'effetto antimicrobico degli scaffold, esso non dovrebbe essere progettato a discapito della biocompatibilità di queste strutture e della loro capacità di promuovere la rigenerazione tessutale. Inoltre, guardando a lungo termine allo sviluppo di scaffold da sfruttare nel futuro prossimo, è sempre più chiaro che queste strutture non dovrebbero basarsi su antibiotici ordinari per la loro attività antimicrobica. Stiamo infatti entrando nella cosiddetta epoca post-antibiotica a causa dell'antibiotico-resistenza dei batteri, che sta rendendo inutili la maggior parte degli antibiotici utilizzati in clinica. La necessità di nuovi antimicrobici risulta quindi evidente, e in questo scenario i peptidi antimicrobici (AMPs) stanno ricevendo crescente attenzione a causa delle loro proprietà antimicrobiche. Tra gli AMPs, quelli ricchi in prolina (PrAMPs) sono di particolare interesse in quanto combinano la potenza antimicrobica degli AMPs con una rassicurante biocompatibilità, evitando problemi di citotossicità che affliggono varie altre classi di AMPs.

Scopo di questo progetto era di caricare PrAMPs ottimizzati razionalmente su scaffold di alginato/idrossiapatite (Alg/HAp) per produrre matrici antimicrobiche che mantenessero la capacità degli scaffold di Alg/HAp di assistere la rigenerazione ossea.

In primo luogo, per rendere i PrAMPs più potenti e per modificare la loro attività antimicrobica per colpire meglio patogeni della chirurgia ortopedica, il PrAMP Bac7(1-16) è stato modificato sostituendo alcuni residui aminoacidici, Successivamente, è stata anche aggiunta una porzione lipidica all'N-terminale del peptide modificato. Solamente il primo approccio ha avuto successo, portando al B7-005, un nuovo PrAMP che mostra attività antimicrobica migliore e più ampia, Dall'altro canto, la lipidazione del B7-005 è stata controproducente, dal momento che non ha migliorato le proprietà antimicrobiche del peptide ma ne ha peggiorato marcatamente la biocompatibilità rispetto alle cellule umane.

Quindi, seguendo un protocollo ben consolidato, sono stati preparati scaffold di Alg/HAp che, previa debiti aggiustamenti iniziali, sono poi stati efficientemente caricati con B7-005 tramite adsorbimento superficiale. Tuttavia, una volta adsorbito sullo scaffold, il peptide rimaneva tenacemente trattenuto dalla struttura e non poteva essere rilasciato in soluzione a causa della forte interazione elettrostatica in essere tra l'alginato e il B7-005. I tentativi di modulare l'interazione elettrostatica riducendo la carica superficiale dello scaffold, usando un chitosano modificato con lattosio, sono stati inutili. Le strutture a base di alginato si sono rivelate quindi scarsamente compatibili con AMPs cationici.

Al fine di preparare scaffold compatibili con il caricamento e il rilascio di B7-005, è stato messo a punto un protocollo per sostituire l'alginato con agarosio durante la preparazione dello scaffold. Sono stati preparati scaffold tridimensionali porosi di agarosio/idrossiapatite (Aga/HAp) mantenendo la proporzione tra polisaccaride e materiale ceramico precedentemente utilizzata per il sistema Alg/HAp. L'imaging SEM e la tomografia microcomputerizzata hanno indicato che gli scaffold Aga/HAp mostravano porosità complessiva, così come la dimensione dei pori e l'interconnessione, simile agli scaffold Alg/HAp. Gli scaffold Aga/HAp sono stati quindi considerati idonei per scopi di rigenerazione ossea.

Gli scaffold Aga/HAp di nuova concezione sono stati caricati con B7-005 mediante liofilizzazione e hanno mostrato un successivo rilascio efficace di peptide. Una linea di cellule ossee umane è stata utilizzata per il test di biocompatibilità, indicando che gli scaffold Alg/HAp sono compatibili con le cellule umane, nonché che potrebbero aderire e proliferare su di essi. Inoltre, è stato poi dimostrato che le cellule possono proliferare

anche su scaffold trattati con B7-005, sebbene la loro velocità di proliferazione fosse ridotta nel periodo iniziale.

Gli scaffold Aga/HAp sono stati ulteriormente analizzati e hanno mostrato un comportamento di rigonfiamento limitato a tempi molto brevi. Le strutture porose hanno mostrato una resistenza meccanica sostanzialmente molto bassa durante le prove di compressione, ma d'altra parte la loro stabilità è stata costante nel tempo, non mostrando segni di degradazione dopo l'incubazione in fluidi corporei simulati fino a 2 mesi.

Infine, è stato dimostrato che gli scaffold B7-005 Aga/HAp possono inibire la crescita di patogeni batterici di rilevanza clinica, sebbene vi sia ancora spazio per un'ottimizzazione volta a migliorare le loro proprietà antimicrobiche.

Nel complesso, i risultati raccolti nel presente lavoro hanno dimostrato che l'agarosio è più adatto dell'alginato per l'uso combinato di polisaccaridi e peptidi antimicrobici cationici. È stato inoltre dimostrato che è possibile sostituire l'alginato con l'agarosio in un protocollo per produrre scaffold porosi tridimensionali, mantenendo diverse proprietà desiderabili dei ben caratterizzati scaffold Alg/HAp.

INTRODUCTION

The bone tissue has remarkable intrinsic regenerative properties, as a consequence of the physiologic constant need for renewal of this tissue, but also as the capability of response to- and repair damages (Dimitriou *et al.*, 2011). After a fracture, the well concerted cascade of phenomena, such as blood clotting, deposition of a cartilaginous callus, together with the finely regulated inflammatory response, angiogenesis and recruitment of mesenchymal stem cells provide an effective reaction to the traumatic events. The subsequent endochondral ossification and the cycles of deposition and re-adsorption of inorganic matrix, in most cases fully restore the integrity and functionality of the injured bone (Einhorn and Gerstenfeld, 2015). However, despite the high efficiency of this healing process, a minority of bone fractures do not heal spontaneously as the consequence of massive bone loss. These complicated conditions, generally occurring when the dimension of the defect surpasses more than twice the diameter of the injured bone, result in what is called a critical bone defect. This means that the lesion cannot be repaired by the body for more than the 10% of its extension during the whole lifespan of the organism (Wang and Yeung, 2017). Critical bone defect are usually the consequence of an extensive trauma, but can be also the result of surgical bone resection for tumour removal, osteonecrosis, severe fragility fractures, infections, and developmental abnormalities (Roddy *et al.*, 2018). Also smaller bone defects can turn critical under the influence of several other factors, *e.g.* anatomic location of the defect, associated biomechanical and soft tissue conditions of the fracture site, as well as systemic and metabolic conditions, age, and other morbidities affecting the proper healing capacity of the organism (Rimondini *et al.*, 2005; Lindsey *et al.*, 2006). Anyhow, whatever may be the origin of the critical defects, their direct consequence is a severe and negative impact on the life-quality of patients. This has as also a reflection on the society and public health due to increased costs for private and public health, but also in terms of reduction of the productivity of patients that may bear long lasting or irreversible physical and psychic consequences (Reichert *et al.*, 2009).

The need to overcome the problematics raised by critical bone defects is evident. Several approaches have been therefore pursued to promote the bone regeneration also under conditions that naturally would not allow the healing of the defect (Wang and Yeung, 2017). Many different kinds of bone substitutes to fill the void in the bone defects were therefore developed, trying to provide for a combination of mechanical support and promotion of bone regeneration for the patients (Khan *et al.*, 2005). Despite their origin, bone fillers should all display the same important biological properties to let the bone grow on their surface or in their pores: osteoconduction, osteoinduction and osteointegration. The graft, to be osteoconductive, should allow the adhesion, proliferation and migration of osteoblast or osteoprogenitor cells within the structure. To be osteoinductive, on the other hand, the draft should promote the differentiation of progenitor stem cells into a bone forming linage and efficaciously promoting the osteogenesis. A third important factor for a graft is the osteointegration, *i.e.* the anchoring of the draft (with the new formed bony tissue) to the native bone of the host, preventing any infiltration of fibrous tissues at the interface that would create undesired skeletal discontinuity (Albrektsson T. and Johansson C., 2001).

Both logically and historically, the first choice for a material answering these requirements has been the bone tissue itself (Fernandez de Grado *et al.*, 2018; Winkler *et al.*, 2018). The grafting of bone tissue is a valuable attempt to treat critical defects. Autologous bone graft offers the great advantage of complete compatibility and efficient osteointegration, allowing to transplant not only the bone matrix, but also the whole cell populations inhabiting the transferred tissue and all the present growth factors. Autograft therefore fulfils also the requirement of osteoinduction. However, the amount of bone tissue that can be transplanted is necessarily limited, and the patient must undergo a double surgical treatment considering both explant and implant, that may leave undesired consequences (Lieberman and Friedlaender, 2005; Roberts and Rosenbaum, 2012). Heterologous bone grafts represent therefore an answer to the broad need of treatments for critical defects, since there is much more availability of material, especially in the last years, thanks to dedicated biobanks. Anyhow, also heterologous transplantations has shadows, for example the immunologic response of the patient toward the implanted tissue, the minor efficiency in promoting the bone regeneration, and the risk (limited but reported) to transfer also pathogens from the donor to the final patient (Lieberman and Friedlaender, 2005; Roberts and Rosenbaum, 2012). The same problems affecting allografts, affects also xenografts, that anyhow,

as a counterweight for their drawbacks, offer an even broader availability of material compared to allograft, given their animal origin (Shibuya and Jupiter, 2015). However, in the end, bone transplantation cannot fully answer the need for solution for critical defects in orthopaedic procedures.

Other approaches were therefore tried over time in order to circumvent the provision problem, and other kinds of bone graft were used. The use of natural compounds to fill the void in bone defects has a long tradition, followed over time by material of synthetic origin (Fernandez de Grado *et al.*, 2018; Winkler *et al.*, 2018). However, in the beginning most often the grafted material simply provided mechanical support, replacing the bone tissue instead of helping its regeneration. This second regenerative aim is in fact much more challenging, and in order to address it, the bone substitute must display specific characteristics in order to satisfy at least the first requirement for bone regeneration, *i.e.* osteoconductivity. To provide therefore an efficient scaffolding activity to promote new bone formation, the grafted bone-substitute should be as similar as possible to the real bony tissue. It should display a three-dimensional structure allowing the cell growth and migration as well as the formation of blood vessels (Sohn and Oh, 2019). To this aim, a porous organization is effective in accommodating the cells incoming from the surrounding environment, as well as in hosting them and consenting their movements. Both phenomena are in fact pivotal events for effective scaffold colonization. More specifically, pores displaying a diameter between 100-350 μm are desirable for bone regeneration, as they display the best efficacy in promoting the deposition of new bony tissue (Bružauskaitė *et al.*, 2016). This represents a further limit in the choice of the material.

In order to promote defect regeneration, the scaffold should also possess biomechanics quite similar to that of the surrounding tissue. This factor is very important to drive proper differentiation of stem cells toward a bony phenotype, and displaying therefore osteoinductive properties (Sohn and Oh, 2019). The mechanic of the graft influences the destiny of the cells that should exploit its scaffolding activity to fill the void of the bone defect. Especially the elastic modulus influences the fluid dynamics into the scaffold, which is of primary importance in providing nutrients and oxygen to the inhabitant cells. Moreover, it is recently becoming more and more clear that the mechano-perception of the surrounding environment by cells plays an important role in determining their fate. The stiffness of the extracellular matrix can indeed influence and drive cell differentiation similarly to other more characterized biochemical factors (Parisi *et al.*, 2018).

This already complicated scenario becomes even more complex considering the influence exerted by the biomaterial itself composing the bone substitute on the cell adhesion and proliferation. As last, moving to a further level of intricacy, to ensure also the osteoinduction, a scaffold should also provide a proper environment and growth factors to trigger the effective subsequent formation of new bone tissue (Sohn and Oh, 2019).

As last, an optimal scaffold should be slowly biodegradable, in order to leave the space for the growing bone tissue while retaining its appropriate supporting role over time during the healing process (Williams, 2008).

The difficulty to find a material combining all these requirements is evident. Therefore, the artificial bone substitutes became extremely attractive, since they allow a reasonable tailoring of the final structure in order to customize the material selecting the desired properties. A plethora of different scaffolds to assist bone regeneration have been proposed following the progresses of tissue engineering and material sciences. Both synthetic and natural compounds have been used to prepare scaffolds for bone regeneration, applying several different techniques, but with the same aim to prepare porous structures satisfying as much as possible the requirements reported above that a scaffold should satisfy. The variety of approaches and products is impressive and has been extensively and nicely reviewed (Karageorgiou and Kaplan, 2005; Bose, Roy and Bandyopadhyay, 2012; Qi *et al.*, 2021).

In the galaxy of porous three-dimensional scaffolds, those composed by polysaccharides represent an appealing compromise between desirable features for bone regeneration, possibility of customization and easiness of preparation. Glycosaminoglycans, chitosan, cellulose and alginate have been broadly used for biotechnological applications and scaffold preparation. These polysaccharides, given also their promising biocompatibility, have been exploited alone, in combination or after chemical modification, according to the desired final result, to produce three-dimensional scaffolds for tissue engineering (Souza *et al.*, 2021). In fact,

the possibility to produce fibres, layers and particularly gels with these polysaccharides, paved quickly the way to the production of porous three-dimensional scaffolds intended for bone regeneration. Among these macromolecules, alginate is one of the best characterized and used polysaccharides (Venkatesan *et al.*, 2015) (Croisier and Jérôme, 2013). Several approaches have been employed to prepare alginate hydrogels, including ionic gelation, thermal gelation, cell crosslinking, chemical crosslinking, and radical polymerization. Then, there are also many possibilities in order to transform the hydrogels in a porous matrix, *e.g.* solvent casting and particulate leaching, foaming, and lastly freeze-drying, which is the most easy procedure to produce three-dimensional porous scaffolds (Sun and Tan, 2013).

However, despite the plenty of opportunities offered by alginate in preparing porous scaffolds, this polysaccharide suffers from poor adhesive properties toward human cells. This deficiency in promoting cell adhesion, and the consequent meagre osteoconductivity, can be circumvented quite easily modifying the alginate itself linking covalently on the polysaccharide chains some components enhancing cells accommodation. Few examples of this approach are the decoration of alginate with RGD peptides or growth factors (Shachar *et al.*, 2011; Sun and Tan, 2013). Otherwise, looking at the use of this material in a bigger picture, cell adhesion not directly to alginate, but to alginate-composed structures, can be enhanced quite easily mixing the alginate with other compounds that are known to promote the settlement of cells. To this aim, alginate was therefore combined with several polymeric compounds (*e.g.* collagen, chitosan, etc.) but also with ceramic compounds. Among these stratagems, very promising results have been obtained in the field of bone regeneration using ceramic-implemented scaffolds composed by a mix of alginate and hydroxyapatite (Venkatesan *et al.*, 2015). Hydroxyapatite has been selected as a good candidate to be mixed with alginate as it is a native component of the bone, and because it has appealing osteoconductive and osteo-inductive properties (Wang and Yeung, 2017). Moreover, this ceramic material had been already used to enhance the mechanic resistance of scaffolds (Zhang and Ma, 1999) and represents a useful source of calcium ions, that can be used for alginate gelation. Alginate/hydroxyapatite porous scaffolds have been deeply described, evaluating the influence of variations in the composition and preparation, and analysing the structure, the mechanical properties and the stability of these objects. Furthermore, the biocompatibility of these structures has been tested using human cell lines. In the end, strong evidence has been produced to support the use of these scaffold to assist the bone-regeneration process. Through the years, a simple pipeline to obtain quite easily alginate/hydroxyapatite was designed, paving the way to further studies and enhancing downstream experimentations (Lin and Yeh, 2004; Turco *et al.*, 2009). Further studies then refined the production of alginate/hydroxyapatite for several purposes, *e.g.* with the aim to obtain peculiar porous structures (Porrelli *et al.*, 2015), to promote their osteo-conductivity by adding in the mix also other cell-adhesive polymers (Sharma *et al.*, 2016; Porrelli *et al.*, 2021), or to endow these structure with antimicrobial activity (Marsich *et al.*, 2013). The detailed description of the many different tailoring performed on alginate/hydroxyapatite scaffolds would however defocus the attention from these scaffolds, that represent a simple but robust and well characterized starting point to analyse the influence of further elements to be introduced into these structures.

Among the previously described tailoring, the attempts to confer antimicrobial activity to alginate/hydroxyapatite scaffolds are now gaining further interest. These (or similar) structures have been implemented with *e.g.* silver nanoparticles (Marsich *et al.*, 2013), with the capability to release nitric oxide (Pant *et al.*, 2019), and with chlorhexidine (Sukhodub *et al.*, 2018). In general, the idea to provide antimicrobial activity to scaffold to be implanted is an attempt to combat surgical implant-associated infections. Biomaterial sciences is therefore moving also toward this direction (Inzana *et al.*, 2016) and this topic will probably gain further importance in the next future. In fact, surgical infections, despite the progresses of the medical practices, remain unfortunately a not neglectable risk for the patients undergoing bone implant procedures. The incidence of infections ranges from 0.5-2% after fixation of closed fractures, but it can reach 30% in open fractures. In the lack of prompt intervention, the local infections may end in severe osteomyelitis whose treatment may need heavy antibiotic therapy and/or secondary surgery. The implant failure, the spreading of the infection to other anatomic districts and even life-threatening bacteraemies are tangible consequences (Trampuz and Zimmerli, 2006). Most often, the pathogen of major concern for orthopaedic surgery is the Gram-positive *Staphylococcus aureus*, responsible of these infections in approximately 60% of the cases.

However, also other microorganisms have been associated to osteomyelitis, *e.g.* the Gram-positive *Staphylococcus epidermidis* and the Gram-negative *Escherichia coli* and *Pseudomonas aeruginosa*. These pathogens are particularly plaguy because of their capability to organize themselves in biofilms that can grow on biotic and abiotic surfaces, including prosthesis and biomaterials used for scaffolds production. Biofilms represent a serious medical problem since they are intrinsically much less sensitive to antibiotics and to the insults of the host immune response, compared with the planktonic form of the same pathogens (Zimmerli and Sendi, 2017). Unfortunately, some of these pathogens are also among the microorganisms that are more prone to become resistant to antibiotics. There is no need to describe therefore how dangerous can be a biofilm composed by antibiotic-resistant pathogens growing on a bone-graft or at its interface with the tissues of the host. The onset of antibiotic-resistant osteomyelitis is therefore an increasing problem that must be faced by clinicians. However, clinicians must be supported by researchers in this fight, since it will be soon impossible to tackle these pathogens using the ordinary antibiotics that are available in hospitals (Yehouenou *et al.*, 2020) and this must be taken in account during the development of antimicrobial scaffold for bone regeneration. It was not by chance therefore that the aforementioned studies, aiming to confer antimicrobial activity to alginate/hydroxyapatite scaffolds, used non-specific antimicrobial agents instead of common antibiotics. This makes sense in the current scenario of antibiotic-resistant infective diseases. Our world is experiencing the unstoppable spreading of pathogens that became insensitive to most (or all) the antibiotics used in clinic. There is therefore the tangible risk to lose the antibiotic therapy within the next future, with severe and worrisome impact on the public health and medicine. The need for new effective and broad-range antimicrobial compounds has become therefore evident (Ventola, 2015a, 2015b).

In the frame of the research for new antibiotics, antimicrobial peptides (AMPs) are in the spotlight due to their promising antimicrobial effects. These natural compounds are attractive for the development of new drugs as they are endowed with immunomodulating properties, but also with a potent direct antimicrobial effect. Most AMPs are small cationic peptides that elicit their mode of action interacting electrostatically with the bacterial membrane. Subsequently, and most often aften a conformational re-arrangement, the AMPs penetrate the phospholipid bilayer destabilizing, permeabilizing or even exerting extensive damages to the bacterial membrane. Microorganisms are then killed by metabolite and ions efflux (Mahlapuu *et al.*, 2016). The description of the specific mechanisms used by AMPs to permeabilize the bacterial membrane does not fall in the aim of this work. However, the relatively non-specific interaction of AMPs with the bacterial envelope (that becomes therefore a massive and diffuse target) allow these peptides to overcome bacterial antibiotic resistance, which relies generally on completely different mechanisms. On the other hand, the targeting of the bacterial envelope make more difficult for microorganisms to develop resistance mechanisms as previously observed for commonly used antibiotics. This feature of AMPs, together with their capability to damage not only planktonic bacterial but also those already organized in biofilms promote the efforts in pushing these molecules toward clinical studies (Magana *et al.*, 2020). Among the possible fields of application for AMPs, not surprisingly there are also osteomyelitis, as well as the use of AMPs for the derivatization of prosthesis or scaffolds in order to prevent bone infections (Kazemzadeh-Narbat *et al.*, 2010; Bormann *et al.*, 2017; Riool *et al.*, 2017; Boix-Lemonche *et al.*, 2020). However, despite significant efforts in the study of AMPs and after also some of these molecules (or their derivatives) entered the pipeline for clinic approval, only very few of them became antibiotics. The main reason of this bottle neck is that AMPs in many cases suffer from limited selectivity for prokaryotic cells and may display undesired cytotoxic effect toward human cells, mainly by damaging also their membranes. The moderate specificity that characterizes the efficient targeting of bacterial cells by AMPs, and that represents an advantage in terms of broad range of antimicrobial effect, can be also a drawback limiting the clinical use of these peptides (Magana *et al.*, 2020).

But this is not the case of all the AMPs. There is a subclass of antimicrobial peptides that often displays very high biocompatibility with mammalian cells, *i.e.* the family of the proline-rich antimicrobial peptides (PrAMPs). These molecules have been identified in several animals, regardless of their phylogenetic relationships, ranging from arthropods to mammals. Despite their origin, PrAMPs share the high content of proline (and arginine) in their sequence (Scocchi, Tossi and Gennaro, 2011). The lack of cytotoxicity displayed by the majority of PrAMPs is the mirror image of their peculiar mode of action, that relies minimally on the

destabilization of the bacterial membrane, which is limited to a secondary mechanism occurring only at high concentration. Several PrAMPs therefore, unlike most AMPs, inactivate microbes mainly by a non-lytic mode of action. These molecules pass the bacterial envelope without exerting any (or significant) damage, and once into the bacterial cytosol they target and block essential bacterial targets. Generally, this mode of action is strictly related to the presence of inner membrane transporters (SbmA and the MdtM complex) expressed by the bacterial species that, not surprisingly, are more sensitive to those antimicrobial molecules. The strictly non permeabilizing PrAMPs, after the active transport by these membrane proteins, once inside the bacterial cell, exert a lethal block of the protein synthesis. This happens by binding and blocking the chaperon DnaK, and most relevantly, the bacterial ribosome. To date, PrAMPs whose mode of action has been revealed at molecular details, have been shown to prevent ribosomes to enter the elongation phase, or sequestering the release factors on the ribosomes, stalling therefore them in the termination phase (Florin *et al.*, 2017; Graf *et al.*, 2017). Generally, PrAMPs targeting primarily the protein synthesis share some sequence portions that are instead not conserved in other PrAMPs, that have been discovered more recently and that are more prone to membrane-permeabilizing activity. These proline-rich membrane-active peptides do not display the usual biocompatibility toward mammalian cells characterizing usually other PrAMPs. They will be no more treated in this context, as any biomedical application for these molecules is at date still far (Mardirossian *et al.*, 2020; Sola *et al.*, 2020; Pacor *et al.*, 2021).

Among the PrAMPs, one of the best characterized molecules is the bovine cathelicidin Bac7. Over the years, this peptide was deeply studied, identifying the shortest portion of its sequence still retaining relevant antimicrobial activity toward pathogens of clinical interest, and describing its mode of action in details. This fragment, Bac7(1-16), composed by the first 16 N-terminal residues of Bac7, displays a mode of action almost exclusively non-lytic, making it very selective toward bacterial cells. As a desirable consequence, the biocompatibility of Bac7(1-16) toward mammalian cells is very high. On the other hand, since this peptide relies almost entirely on the non-lytic bactericidal mechanism, it is strictly dependant on the presence of the transporters on the bacterial envelope in order to exert its antibacterial activity. This strict reliance of Bac7(1-16) on the expression of proteins such as SbmA or the MdtM complex (or their homologues) by pathogens narrows the spectrum of activity to a limited number of Gram-negative peptides. Even though the bacterial species targeted by Bac7(1-16) encompass clinically relevant pathogens like *Escherichia coli*, *Klebsiella pneumoniae*, *Salmonella enterica* spp. and *Acinetobacer baumannii*, a broader spectrum of activity would be desirable for this molecule (Benincasa *et al.*, 2004; Podda *et al.*, 2006, 2006; Mattiuzzo *et al.*, 2007; Scocchi, Tossi and Gennaro, 2011; Krizsan, Knappe and Hoffmann, 2015; Mardirossian *et al.*, 2020). The targeting by a PrAMPs also of pathogens like *Staphylococcus aureus* and *Pseudomonas aeruginosa*, commonly less affected by native non-lytic PrAMPs (Benincasa *et al.*, 2004; Runti *et al.*, 2017), would make it a very interesting lead compound to design new antimicrobial drugs. Moreover, since the transporters exploited by Bac7(1-16) as "trojan horse" to enter the bacterial cytosol are not essential for the life of microorganisms, it would be quite easy for bacteria to naturally develop resistance toward this antimicrobial peptide (Narayanan *et al.*, 2014). The dependency of Bac7(1-16) on the active transport by bacteria should therefore be circumvented in order to push forward this molecule in the pipeline for the development of new antibiotics. The research is moving also in this direction, attempting modification of the sequence of the peptide and its conversion into a lipo-peptide (Mardirossian *et al.*, 2020; Armas *et al.*, 2021)

AIM OF THE PROJECT

Porous scaffolds for bone regeneration should be implemented with new-generation antimicrobials in order to be safely used in the age of the bacterial antibiotic resistance. An antimicrobial peptide is therefore an optimal candidate to confer antimicrobial properties to these three-dimensional structures. On the other hand, alginate/hydroxyapatite scaffolds are a very good model to try this combination. They are efficient in promoting bone regeneration, well characterized, and display negative electrostatic charge, that may help the loading of the peptide on the scaffold. Proline-rich antimicrobial peptides on the other hand are potent and safe antibacterial compounds, however in order to shield scaffolds intended for bone regeneration from main pathogens, their spectrum of action should be broadened.

Aim of this project was to modify the proline-rich peptide Bac7(1-16) to expand its antimicrobial range of activity, and then to load it on alginate/hydroxyapatite scaffold, in order to develop antimicrobial and biocompatible scaffolds for bone regeneration.

MATERIAL AND METHODS

Peptides synthesis and purification

The B7-005 and LipoB7-005 were purchased as chloride-salt from the NovoPro company (Shanghai, China). The molecules were synthesised on solid-phase using Fmoc chemistry, purified to ≥95% by reverse-phase HPLC and their identity was confirmed by mass spectrometry. B7-005 was then solved in sterile water and quantified by UV-spectrophotometry upon proper dilution according to the Lambert-Beer equation, calculating its ε_{280} and ε_{214}. LipoB7-005 was solved in DMSO and quantified by UV-spectrophotometry upon proper dilution according to the Lambert-Beer equation, calculating its ε_{280} using the online tool "ProtParam". The ε_{214} was calculated using the in house developed software "ConCalc", as reported in Mardirossian *et al*. 2020. The quantified stocks were then stored at -20°C.

Alg/HAp scaffold preparation

Alginate (2% w/v)/Hydroxyapatite (3% w/v) scaffolds were prepared as described in Turco *et al*. 2009. Briefly, an alginate solution was prepared solving at room temperature an adequate polymer amount (LF10/60, Novamatrix) overnight under agitation in a deionized water volume corresponding to the 70% (v/v) of the desired final volume of gel. The day after, an adequate amount of micrometric powder of hydroxyapatite (Sigma) was dispersed under vigorous stirring for 30 min. in a deionized water volume corresponding to the 20% (v/v) of the desired final volume of gel. The HAp suspension was then added to the Alg solution and mixed under vigorous agitation using a magnetic stirrer for approx. 2 hours. Finally, an adequate amount of glucono-δ-lactone (Sigma) to reach the final concentration of 60 mM was solved in a deionized water volume corresponding to the 10% (v/v) of the desired final volume of gel and immediately added to the Alg/HAp. After quick vigorous stirring (no more than 60 sec.), the mix was poured into a 24-wells plate (Sarstedt) filling completely the wells. The plate was then capped and let undisturbed overnight to allow alginate gelation. The day after, the plate was sealed with parafilm and double sealed into a plastic bag, then frozen under controlled conditions to -20°C, decreasing the temperature 1°C/4 min by immersion in a liquid cryostat (circulating bath 28L, VWR, Radnor, PA, USA) using silicon oil as refrigerant fluid. After freezing, the plate was freeze-dried with an ALPHA 1-2 LD plus freeze-drier, CHRIST, (Osterode am Harz, Germany) for 48 hours. In order to expose the porosity of the dried scaffolds, they were cut with a scalpel to remove their very distal portions, cored using a circular scalpel with a diameter of 8 mm and their hight was equalized to 10 mm.

To remove any leftover reagent, each scaffold was washed four times in the wells of a 24-wells (Sarstedt) with 2 mL of $CaCl_2$ for 15 min, then removed by the solution, whose excess was drained from the scaffold sitting them on paper towels. Similarly, scaffolds were rinsed with 2 ml of water for 5 min, washed in PBS (pH 7.2) for 5 min to equilibrate their pH, rinsed with 2 ml of water for 5 min. Subsequently, scaffolds were partially dehydrated moving them for 5 min in 70% (v/v) ethanol, dried then in the air for 5 min, frozen at -20°C and freeze-dried overnight. Scaffold were then stored for subsequent use in sealed containers.

Loading of B7-005 on Alg/HAp scaffolds

Scaffolds prepared as previously described (approx. 25 mg/ each) were soaked in 2 mL of an aqueous solution of B7-005 to a final concentration of 128 µg/mL in the wells of 24-wells plate (Sarstedt). Some scaffolds were soaked in water only, as a control to check that no more undesired chemicals were released by the scaffolds. The plate was then incubated at room temperature under mild agitation. The absorbance of 1 mL of the supernatant of each scaffold was then assessed overtime transferring it in a quartz cuvette and reading at 280 nm. The solution was then re-added in the corresponding well. The peptide in the supernatant was quantified according to the Lambert-Beer equation. After 4 hours, once assessed that there was no more peptide in the supernatant, the scaffolds were freeze-dried to remove the water and stored for subsequent uses in sealed

containers at -20°C. The experiments were performed using 3 scaffolds for any tested condition, in two independent experiments (n=6).

Release of B7-005 from Alg/HAp scaffolds

Peptide-loaded scaffolds prepared as above were soaked in 2 mL of sterile PBS and incubated at 37°C in the wells of 24-wells plate (Sarstedt). Scaffolds loaded with water only were used as a control and to set the blank. The absorbance of 1 mL of the supernatant of each scaffold was then assessed overtime transferring it in a quartz cuvette and reading at 280 nm. The solution was then re-added in the corresponding well. The peptide in the solution was quantified according to the Lambert-Beer equation. The experiments were performed using 3 scaffolds for any tested condition, in two independent experiments (n=6). after 72 hours of incubation, NaCl was added to all the wells containing the scaffolds to the final concentration of 1M. The plate was incubated for 2 hours at 37°C then the peptide in the supernatant was quantified as reported above.

CTL-coated Alg/HAp scaffolds

A 0.2 % (w/v) aqueous solution of lactose-modified chitosan (CTL) was prepared solving the polymer at room temperature under stirring and bringing the solution to pH 7.2 with NaOH and sterilized by filtration at 0.22 µm. Alg/HAp scaffolds, prepared as previously described, were soaked in 1 mL of 0.2 % CTL for 4 hours in the wells of a 48-wells plate (Sarstedt). Scaffolds were then removed from the plate, the excess of CTL solution was drained sitting the scaffolds for 1 min. on a sterile gauze. Scaffolds were frozen at -20°C, freeze-dried for 24 hours. Lyophilized scaffolds were stored for subsequent uses in sealed containers at -20°C. CTL-coated scaffolds were loaded with B7-005 according to the protocol reported above and the release of the peptide was assessed similarly but limiting the time to 48 hours. 3 scaffolds were used for each condition (n=3). Un-coated Alg/HAp scaffolds were used as a blank during UV- quantification of B7-005.

Preparation of Aga/HAp scaffolds

Adequate amount of agarose (Sigma) to reach the final concentration of 2% (w/v) was melted in a water volume corresponding to the 70% (v/v) of the desired final volume of gel using a microwave oven set to 450 W, preventing the solution from boiling. In parallel, an adequate amount of micrometric powder of hydroxyapatite (Sigma) was dispersed under vigorous stirring for 30 min in a water volume corresponding to the 30% (v/v) of the desired final volume of gel and heated as described above. After complete dissolution of agarose, the HAp suspension was then added to the agarose solution and mixed under vigorous agitation using a magnetic stirrer for approx. 30 min, allowing in the meantime the solution to cool down to 60°C. Once reached this temperature, the mix was aliquoted in the wells of a 48 wells-plate (Sarstedt), covered and let to gel undisturbed at room temperature for 1 hour. Once gelation was complete, the plate was sealed with parafilm and double sealed into a plastic bag, then frozen under controlled conditions to -20°C, decreasing the temperature by 1°C/4 min by immersion in a liquid cryostat (circulating bath 28L, VWR, Radnor, PA, USA) using silicon oil as refrigerant fluid. After freezing, the plate was freeze-dried with an ALPHA 1-2 LD plus freeze-drier, CHRIST, (Osterode am Harz, Germany) for 48 hours. In order to expose the porosity of the dried scaffolds, they were cut with a scalpel to remove their very distal portions, and their hight was equalized to 5 mm.

Loading and release of B7-005 with Aga/HAp scaffolds

To load the peptide on Aga/HAp scaffolds (theoretically 128 µg each, therefore 6.4 µg B7-005/ mg scaffold), 100 µL of an aqueous solution containing 128 µg of B7-005 were dropped on scaffolds prepared as above, in order to get the scaffold homogeneously wet but paying attention that all the fluid was adsorbed and retained

by the porous structure. The scaffolds were then frozen at -20°C, then freeze-dried for 24 hours and stored at -20°C up to further experimentation.

The release of B7-005 was assessed soaking the peptide-loaded scaffolds prepared as above in 2 mL of sterile PBS at 37°C in the wells of 24-wells plate (Sarstedt). Scaffolds loaded with water only were used as a control and to set the blank. The absorbance of 1 mL of the supernatant of each scaffold was then assessed overtime transferring it in a quartz cuvette and reading at 280 nm. The solution was then re-added in the corresponding well. The peptide in the solution was quantified according to the Lambert-Beer equation. The experiments were performed using 3 scaffolds for any tested condition, in two independent experiments (n=6).

Scanning electron microscopy of Aga/HAp scaffolds

For SEM analysis, samples were mounted on aluminium stubs with a carbon double-sided tape. Scaffolds were then gold sputtered with a Sputter Coater K550X (Emitech, Quorum Technologies Ltd, UK). The microimaging of scaffolds was performed with a Scanning Electron Microscope Quanta250 (FEI, Oregon, USA.), in high vacuum, in secondary electron mode, with 30 kV of tension and 10 mm of working distance.

Micro-computed tomography of Aga/HAp scaffolds

X-ray microcomputed tomography of scaffolds was performed using a custom-made cone-beam system called TOMOLAB (Elettra-Sincrotrone, Trieste, Italy). Samples were put onto the turn table of the instrument and acquisitions were performed using the following parameters: distance source-detector (F_{DD}), 250 mm; distance source-sample (F_{OD}), 80 mm; magnification, 3.1x; binning, 2×2; resolution, 8 μm; tomography dimensions (pixels), 2004×1335; slices dimensions (pixels), 1984×1984; number of tomographies, 1440; number of slices, 1332; E = 40 kV, I = 200 μA; exposure time, 1.5 s. The process of slices reconstruction and the correction of beam hardening and ring artifacts were performed using the commercial software Cobra Exxim. Input projections and output slices are represented by files (one file per projection and one file per slice) using arrays of 16-bit integers. The slices segmentation was performed according to the Otsu's method (Otsu et al., 1979), using the software Fiji (Schindelin et al, 2012). BoneJ plugin (Doube et al., 2010) implemented on Fiji software was then used to analyse the samples after segmentation.

Swelling test of Aga/HAp scaffolds

Dry Aga/HAp scaffolds (8, n=8) were weighted and submerged with 4 ml PBS in the wells of a 12-wells plate (Sarstedt). At each timepoint, scaffolds were gently removed from PBS with tweezers and put for 10 seconds on 8 layers of paper towel to remove the excess of PBS permeating the structure. Scaffolds were then weighted again, and their variation of weight calculated as the percentage of their dry weight. Subsequently scaffolds were soaked again in the same PBS-containing wells.

Mechanical characterization of Aga/HAp scaffolds

Dry scaffolds were tested with a Universal Testing Machine (GaldabiniSun500, Galdabini, Italy) coupled with a 100 N load cell. A constant deformation of 1 mm/min was exerted until a 4 mm maximum displacement. To test wet scaffolds, the samples were immersed beforehand in PBS for 10 minutes (according to the swelling capacity of the scaffolds, see above) and then analysed with a Dynamic Mechanical Analysis (DMA) system (Electroforce 3300, TA Instruments, New Castle, DE, USA) equipped with a 22 N load cell. A constant compression speed of 1 mm/min was applied to the scaffolds up to a maximum displacement of 3 mm. A total of 8 samples was averaged for each examined condition. The stress-strain curves obtained were used to estimate the elastic modulus (E), calculated in the 2-5% strain interval (within the linear behaviour of the

material), the stress value at which the sample reaches the 50% of deformation (σ[50% strain]), and the toughness of the biomaterial.

Stability test of Aga/HAp scaffolds

Dry Aga/HAp scaffolds were weighted and submerged with 2 mL of simulated body fluid (SBF) (Kokubo and Yamaguchi, 2016) in the wells of a 24-wells plate (Sarstedt), subsequently sealed with parafilm and closed in a plastic bag to prevent evaporation. The plate was then incubated at 37°C. At each timepoint, the SBF was removed and 2 ml of mQ-water were gently added to the wells in order to wash any leftover of SBF and soluble salts still permeating the scaffolds. After 5 min. the water was removed, the scaffolds frozen at -20°C and freeze-dried for 24 hours. Once dried, scaffolds were weighted again, and their variation of weight calculated as the percentage of their dry weight before the incubation. Independent groups of 4 scaffolds were used for each timepoint to avoid multiple soaking/drying steps.

Bacterial Cultures

In this work, the following bacterial strains were used: *Escherichia coli* BW25113, *Escherichia coli* BW25113Δ*sbmA* (JW0368-1, KEIO collection42), *Escherichia coli* ATCC 25922, *Enterobacter cloacae* ATCC 13047, *Staphylococcus aureus* ATCC 25923, *Klebsiella pneumoniae* ATCC 700603, *Acinetobacter baumannii* ATCC 19060, and *Pseudomonas aeruginosa* ATCC 27853, *Enterococcus faecium* ATCC 19434. All the bacterial strains were grown overnight at 37 °C in Müller−Hinton broth (MHB, Difco) with shaking (140 rpm). The day after, bacterial cultures were diluted 1:40 using new MHB and incubated at 37 °C with shaking (140 rpm) up to midlog phase, therefore when an absorbance at 600 nm ≈ 0.3 was reached. Kanamycin (50 μg/mL) was added to the medium only for *E. coli* BW25113Δ*sbmA*.

Minimum inhibiting concentration assay

Bacterial cultures were grown as above to the mid-log phase and subsequently diluted to 5×10^5 colony-forming units (cfu)/mL in MHB. The peptides were diluted in the same medium to the concentration of 128 μM (or μg/mL), and 100 μL of peptide solution were added to the first wells of a round-bottom 96-well microtiter plate (Sarstedt), then serially twofold diluted in in successive wells in 50 μL of MHB. Subsequently, 50 μL of bacterial suspension 5×10^5 cfu/mL were added to each well. This halved both the final bacterial load to 2.5×10^4 cfu/well and the peptide concentration in the wells. As a control for bacterial growth, in some wells bacteria were added to 50 μL of MHB only. 100 μL of MHB without bacteria were used to check the medium sterility. The plate was sealed with Parafilm to reduce evaporation and subsequently incubated overnight at 37 °C (approx. 18 h). The MIC was calculated as the lowest concentration of peptide preventing bacterial growth in the wells evaluated by visual inspection as the first clear well. Data are reported as median of independent experiments repeated three times or four times in case of uncertain values.

Antimicrobial effect of Aga/HAp scaffolds

Sterile Aga/HAp scaffolds, prepared and loaded with B7-005 as above, were soaked in 2 mL of MH medium containing bacteria at the concentration of 2.5×10^5 CFU/mL in the wells of a 24-wells plate (Sarstedt). As a reference, identical scaffolds, but loaded with sterile water only, were soaked in the same bacterial suspension or in MH medium only, to assess the sterility of the scaffolds. The plate was then incubated at 37°C overnight for 18 hours. The day after, the absorbance at 600 nm of 1 mL of each well was measured using a spectrophotometer. The inhibition of bacterial growth was calculated as a percentage comparing the absorbance of the bacterial suspensions growing in the presence of scaffolds loaded or not with the B7-005 peptide. Two independent experiments were performed.

B7-005 and LipoB7-005 biocompatibility assays

Biocompatibility assays on the human cell line MEC-1 (lymphocytes B precursor cells) were performed using the tetrazolium salts test (MTT), exposing cells to peptides or sterile water as a control at 37 °C and 5% CO_2. MEC-1 cells were grown in RPMI (Sigma) + 10% fetal bovine serum (Sigma) + 2 mM glutamine (Sigma) + 100 U/mL penicillin (Sigma) + 100 μg/mL streptomycin (Sigma). After count, cells were diluted to 2×10^6 cell/mL. Twofold serial dilutions of the peptides were set up in the wells of a 96-flat-bottom microtiter plate (Euroclone), in a final volume of 50 μL of cell growth medium. Subsequently, then 10^5 cells were put in each well in a volume of 50 μL, reaching a final volume of 100 μL/well. Sterile water was added to untreated controls. After 20 h of exposure to the peptides at 37 °C and 5% CO_2, 25 μL of MTT in PBS was added to each well (final concentration = 1 mg/ml). The plate was incubated 4 h at 37 °C in the dark. Then 100 μL of Igepal (Sigma-Aldrich) 10% v/v in 10 mM HCl (w/v) were added to each well and the plate was incubated at 37 °C and 5% CO_2 overnight. After approx. 18 h, a plate-reader spectrophotometer Nanoquant infinite M200pro (Tecan) was used to quantify the A_{570nm} of the wells. The cytotoxicity of the peptide was expressed as a percentage, calculated comparing the A_{570nm} of the treated samples with that of the untreated control. Data are the average ± standard deviation of three independent experiments (n = 3).

Biocompatibility assays on the human cell line MG-63 (osteosarcoma) were performed using the Alamar blue test, exposing cells to B7-005, or sterile water as a control, at 37 °C and 5% CO_2. MG-63 cells were grown in DMEM-High glucose (Sigma) + 10% fetal bovine serum (Sigma) + 2 mM glutamine (Sigma) + 100 U/mL penicillin (Sigma) + 100 μg/mL streptomycin (Sigma). After count, cells were diluted to 1.6×10^5 cell/mL, and 100 μL of cell suspension were put in the wells of a 96-flat-bottom microtiter plate (Euroclone). The plate was incubated overnight at 37 °C and 5% CO_2 to allow cell adhesion. Twofold serial dilutions of the peptides were set up in the empty wells of the same plate, in a final volume of 120 μL of cell growth medium. The exhaust medium of the cell-containing wells was removed and substituted with 100 μL of B7-005 solutions previously described. Sterile water instead of peptides were used for untreated controls. After 24 h of incubation at 37 °C and 5% CO_2, the medium containing the peptide was removed, the wells rinsed with 150 μL of PBS. Subsequently, new DMEM-High glucose containing resazurin (dilution 1:30 of the commercial solution Tox8, Sigma) was added to each well. The plate was incubated 4 h at 37 °C in the dark. 100 μL of the supernatant of each well were transferred into the wells of a flat-bottom black 96-wells and the fluorescence was evaluated using a FLUOStar Omega spectrofluorometer (BMG-Labtech), with an excitation wavelength of 544 nm and emission wavelength of 590 nm. The mixture AlamarBlue-DMEM-high glucose was used as a blank. Data are the average ± standard deviation of three independent experiments performed as technical triplicates (n = 9).

The biocompatibility of LipoB7-005 was calculated similarly with Alamar Blue, however some further controls were setup exposing cells to the same DMSO amount transferred in the wells with the lipopeptide (and further dilutions). Data are the average ± standard deviation calculated on a technical triplicate (n = 3).

Cell membrane permeabilization on the human cell line MG-63 (osteosarcoma) were performed using the LDH-release test, exposing cells to LipoB7-005, DMSO or sterile water as a control at 37 °C and 5% CO_2. MG-63 cells were grown, seeded and exposed to LipoB7-005 as previously described for the Alamar blue. The further passages have been performed according to the instruction of the supplier of the LDH-release kit (CytoTox 96® Non-Radioactive Cytotoxicity Test, Promega). After the final incubation, 100 μL of the supernatant of each well were transferred into the wells of a flat-bottom 96-wells microtiter and evaluated using a FLUOStar Omega spectrofluorometer (BMG-Labtech), measuring not only the supernatant but also few dilutions of it, to avoid very strong signals and in order to record values within the linear range of the instrument. Data are the average ± standard deviation calculated on a technical triplicate (n = 3).

Assessment of cell proliferation on Aga/HAp scaffolds

Aga/HAp scaffolds prepared as above were sterilized by soaking overnight in absolute ethanol. The day after, scaffolds were removed from ethanol with sterile tweezers and aseptically dried aseptically in the air under a cell-culture hood. Scaffolds were then loaded as reported above with 6.4 µg B7-005/ mg scaffold, or with sterile water only as a control.

Treated and untreated scaffolds were put in the wells of a 24wells-plate (Sarstedt) and soaked with 1 ml of complete cell culture medium DMEM-high glucose for 30 min. Subsequently, 32.000 MG-63 cells resuspended in a final volume of 120 µL were slowly added dropwise on the top of the scaffold, allowing each drop to be adsorbed by the porosity of the scaffold before adding another-one. Scaffold were incubated for 1 hour, then another ml of DMEM-high glucose was slowly added to each well, avoiding to disturb or move the scaffold, that were subsequently incubated overnight. The day after all the scaffolds were moved in the wells of another 24-wells plate containing 2 mL of fresh DMEM-high glucose, to get rid of any cells that was not attached on the scaffold but decanted on the bottom of the well after the seeding. This was the starting point of the proliferation kinetic. Scaffolds were moved similarly to new plates every week.

For each time-point, 3 B7-005-loaded, 3 untreated scaffolds, and 1 void scaffold (not seeded with cells) were placed in the wells of a 48-wells plate containing 500 µL of DMEM-high glucose containing Alamar Blue (Tox8, Sigma) diluted 1:30. The plate was incubated in the dark for 4 hours at 37°C, 5% CO_2, then the scaffolds were squeezed 10 times using a tip to redistribute any reacted Alamar Blue trapped into the scaffold. Subsequently, 100 µL of the supernatant were transferred into the wells of a flat-bottom black 96-wells and the fluorescence was evaluated using a FLUOStar Omega spectrofluorometer (BMG-Labtech), with an excitation wavelength of 544 nm and emission wavelength of 590 nm. The mixture AlamarBlue-DMEM-high glucose was used as a blank.

RESULTS

Design of new derivatives of the PrAMP Bac7(1-16)

In the frame of a project aiming at the characterization and amelioration of PrAMPs, the screening of several derivatives of the PrAMPs Bac7(1-16) bearing the substitution of a single residue, demonstrated that some sequence modifications improved the antimicrobial effect of the native peptide. Some of these substitutions were selected and combined to design five new Bac7(1-16) derivatives, in the attempt to exploit additive or synergic effects of these modification. The expected results were an improvement of the antimicrobial activity of the new peptides with respect to the original molecule. Looking at the sequences of the derivatives, in most cases a proline was replaced by a tryptophan (P7W in B7-005, P13W in B7-003, P15W in B7-002, -004, -005) or by an arginine (P5R in B7-004, -005), and an arginine was replaced by a tryptophan (R1W in B7-001, -003, -004, -005) (Table 1,(Mardirossian *et al.*, 2020))

Table 1. Bac7(1-16) derivatives designed combining previously identified single-residue modifications to improve the antimicrobial activity of the native peptide. Bold indicates the residues substitutions with respect to the original peptide. Adapted from (Mardirossian *et al.*, 2020).

Peptide	Sequence
Bac7(1-16)	RRIRPRPPRLPRPRPR
B7-001	**W**RIRPRPPRLPRPRPR
B7-002	RRIRPRPPRLPRPR**W**R
B7-003	**W**RIRPRPPRLPR**W**RPR
B7-004	**W**RIR**R**RPPRLPRPR**W**R
B7-005	**W**RIR**R**R**W**PRLPRPR**W**R

Selection of the antimicrobial peptide B7-005

To evaluate the antimicrobial activity of the new derivatives and to identify any advantage with respect to the native Bac7(1-16), minimum inhibiting concentration (MIC) assays were performed testing these compounds on a panel of clinically relevant pathogens. Bac7(1-16) was assessed simultaneously as a comparison. Moreover, to evaluate any modification of the mode of action of the derivatives compared to the original PrAMP, the peptides were tested also on a *E. coli* strain lacking the inner membrane transporter SbmA. This protein is in fact necessary to internalize the natural PrAMPs and therefore partially responsible of their antimicrobial activity.

Among the tested peptides, B7-005 displayed the broader spectrum of activity, encompassing also *S. aureus* and *P. aeruginosa*, pathogens unaffected by the native Bac7(1-16). Although no significant improvement of the *per se* antimicrobial activity of B7-005 was observed toward the model organism *E. coli* and *K. pneumoniae*, the MIC of the peptide toward *A. baumannii* was promisingly lower. Interestingly, B7-005 did not decrease markedly its antimicrobial activity toward *E. coli* BW25113 in the absence of the SbmA transporter (*E. coli* BW25113Δ*sbmA*), suggesting that the peptide can at least partially evade the dependency from this membrane protein for its mode of action (Table 2, (Mardirossian *et al.*, 2020)).

Table 2. Minimum inhibitory concentration (MIC) of Bac7(1-16) and derivatives toward a panel of bacterial species. Adapted from (Mardirossian *et al.*, 2020)

Bacteria	Peptides MIC (µM)					
	Bac7(1-16)	**B7-001**	**B7-002**	**B7-003**	**B7-004**	**B7-005**
***E. coli* BW25113**	3	1	1	2	2	2
E. coli* BW25113Δ*sbmA	16	12	4	16	3	4
***K. pneumoniae* ATCC 700603**	4	16	2	8	4	2
***A. baumannii* ATCC 19606**	32	32	12	32	32	4
***P. aeruginosa ATCC* 27853**	> 64	> 64	> 64	> 64	64	32
***S. aureus ATCC* 25923**	> 64	> 64	> 64	> 64	32	12

Biocompatibility of the peptide B7-005

B7-005 displayed promising antimicrobial activity, however the biocompatibility of all the newly designed B7-peptides was still unknown. To have a first indication if these molecules had undesired cytotoxic side effects toward human cells, they were administered to cells of the human cell line MEC-1 (B-lymphocyte leukemia). No statistically significant toxicity was identified under any tested conditions, although B7-005 at 64 µM displayed variability in the cell viability, and this may represent the first indication of putative cytotoxicity at higher concentrations of peptide (Figure1). However, B7-005 exerted its antimicrobial activity already at low concentration (see Table 2), therefore it represented the best compromise between antimicrobial efficacy and biocompatibility (Mardirossian *et al.*, 2020).

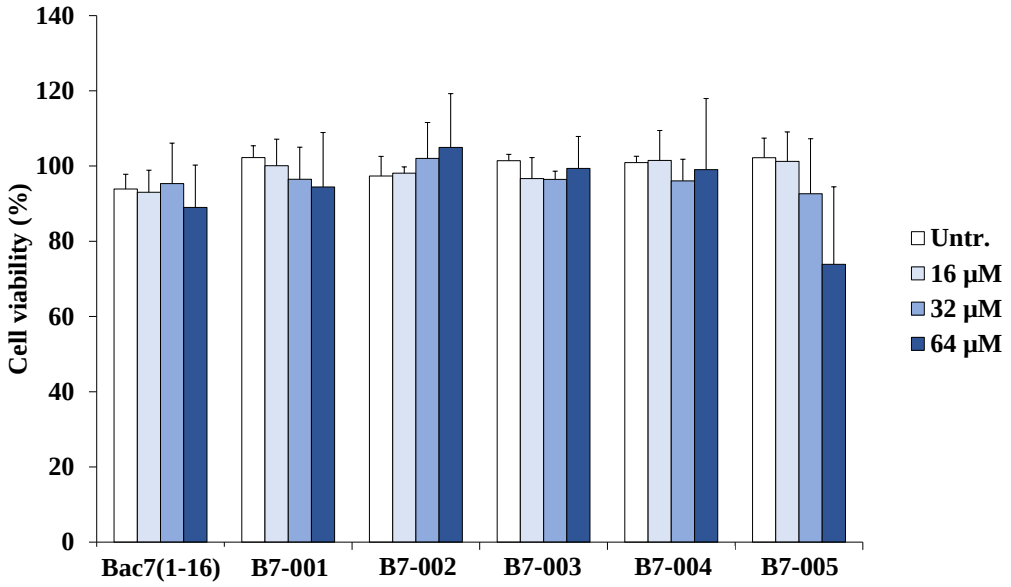

Figure 1. Biocompatibility of Bac7(1-16) and derivatives with MEC-1 cells. The cell viability was assessed by MTT assay and reported as percentage of an untreated control (Untr.), receiving sterile water instead of peptide. Error bars represent the standard deviation calculated on the average of 3 independent experiments (n=3) (modified from Mardirossian 2020). Student t-test.

All these Bac7(1-16) derivatives were further characterized investigating their mode of action in a parallel project (Mardirossian 2020). On the other hand, since these preliminary data on B7-005 were encouraging, the

peptide was considered a good candidate to be loaded on scaffolds for tissue engineering, in order to provide them with antimicrobial activity and discourage the onset of surgical infections after implant.

The aim of the project was to load the antimicrobial component on scaffolds designed for bone regeneration, therefore a first indication of the compatibility of B7-005 with cells approximating the bone tissue was mandatory. A cell viability test was set up exposing the MG-63 cell line (human osteosarcoma) to increasing concentrations of peptide. Because the final application of this peptide should have been its application in the biomaterial field, for the biocompatibility assay as well as for further experimentation, the concentration of B7-005 was reported in µg/mL. No statistically significant toxicity of B7-005 was observed toward MG-63 cells up to the higher tested concentration, *i.e.* 128 µg/mL, corresponding to approximately 55 µM (Figure 2).

To cite further advantages of B7-005 for subsequent applications, the peptide was rich in tryptophans, therefore easily trackable using UV spectrophotometry and its aminoacidic sequence was short (and therefore also relatively unexpensive, compared to other AMPs).

This encouraged the use of B7-005 for further applicative experiments and therefore to be loaded on scaffolds, in this case, alginate/hydroxyapatite (Alg/HAp) porous scaffolds (Turco 2009).

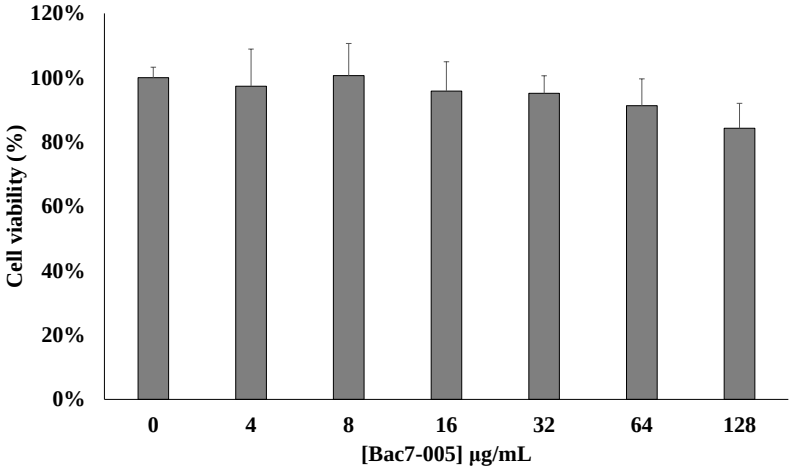

Figure 2. Biocompatibility of B7-005 with MG-63 cells. The cell viability was assessed by Alamar blue assay and reported as percentage of an untreated control, receiving sterile water instead of peptides. Error bars represent the standard deviation calculated on the average of 3 independent experiments performed in technical triplicate (n=9). Student t-test.

Lipidization of B7-005 to improve its antimicrobial activity

There is evidence that antimicrobial lipopeptides exert potent microbicidal activity toward Gram-positive bacteria (e.g. Armas *et al.*, 2019) and this has been extended also to PrAMPs (Domalaon *et al.*, 2018; Armas *et al.*, 2021). We applied therefore a similar approach to B7-005 with the aim to further improve its antimicrobial effect toward *S. aureus* or other Gram-positive pathogens. The LipoB7-005 was synthesised linking by amide bond a dodecanoic acid to the N-terminus of B7-005. Minimum inhibiting and bactericidal concentration assays (MIC and MBC, respectively) were performed to evaluate the antimicrobial potential of the new compound using in parallel reference strains of *S. aureus* and *E. coli*. No improvement was observed in the antimicrobial effect of the lipoB7-005 toward *S. aureus* with respect to the native molecule. On the other hand, LipoB7-005 displayed worse inhibiting and killing effect toward *E. coli* compared to B7-005 (Table 3). From an antimicrobial point of view, no advantage was therefore observed after the lipidation of the B7-005.

Table 3. Minimum inhibitory (MIC) and bactericidal (MBC) concentrations of B7-005 and LipoB7-005 toward the reference strains *E. coli* ATCC 25923 and *S. aureus* ATCC 25922. Data are the median of three independent experiments (n=3).

	MIC (µg/mL)		MBC (µg/mL)	
	B7-005	LipoB7-005	B7-005	LipoB7-005
E. coli ATCC 25923	4	32	8	32
S. aureus ATCC 25922	32	32	32	32

In parallel, the biocompatibility of the LipoB7-005 was explored. To this aim, cell viability assays were performed using the Alamar Blue assay on MG-63 cells exposed to the lipopeptide and to the native peptide. Since lipopeptides generally display relevant affinity for biological membranes, also an LDH-release assay was performed. This allowed to further investigate the biocompatibility of the new compound collecting at the same time very preliminary hints about any membrane-permeabilizing activity. The Alamar blue assay indicated that LipoB7-005 started to decrease the cell viability already at 32 µg/mL (Figure 3A), indicating a lower biocompatibility than the B7-005. The LDH release assay gave results consistent with the Alamar Blue assay, indicating that LipoB7-005 induced a slight permeabilization of the cell membrane at 16 µg/mL that turned then massive at 32 µg/mL and complete at 64 µg/mL, indicating also in this case that LipoB7-005 was not very biocompatible (Figure 3B). These results induced to speculate that the cell permeabilization observed in Figure 3B may be also the cause of the drop in cell metabolism observed in Figure 3A, rather than a mere unspecific consequence of the cell death.

However, taken together, these results indicated that the lipidation of B7-005 ended in a molecule whose biocompatibility was lower compared to that of the native molecule. On the other hand, the LipoB7-005 did not displayed more potent antimicrobial activity than the native peptide. For these reasons, the LipoB/-005 was discarded and no more used for any experimentation.

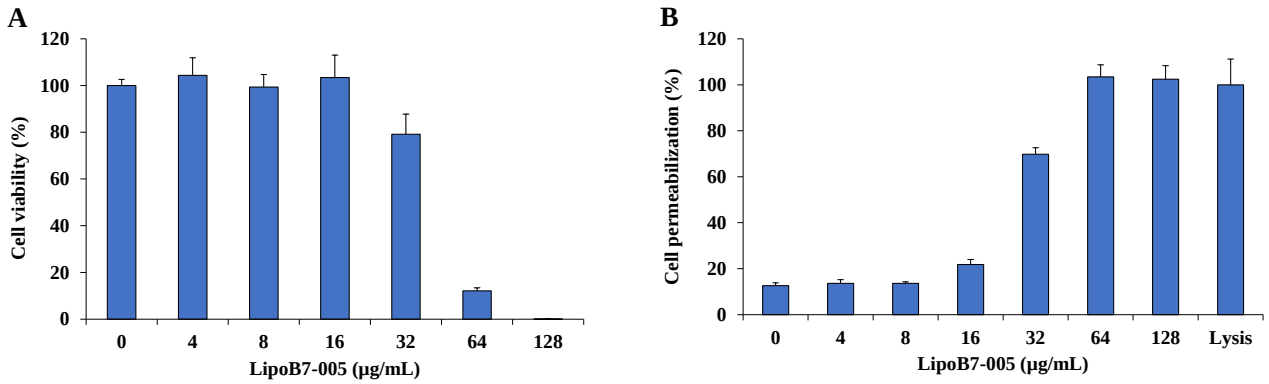

Figure 3. Cell viability assay on MG-63 cells exposed at LipoB7-005 for 24 hours. A) Alamar blue assay. B) LDH-release assay. Error bars are the standard deviation calculated on the average of an internal triplicate (n=3).

Loading of B7-005 on Alg/HAp scaffolds

Since the LipoB7-005 gave not interesting results, B7-005 remained the best candidate molecule to be loaded on the scaffolds for bone regeneration. Alginate/Hydroxyapatite (Alg/HAp) scaffolds have been characterized in detail and represent simple but still effective structures to help the healing of bone defects. For this reason, Alg/HAp scaffolds were selected for downstream experiments regarding the loading and the release of the

most promising peptide, *i.e.* B7-005, in this case. Given the positive net charge of B7-005, it had been supposed that it should be easily adsorbed on the anionic scaffolds by simple electrostatic attraction and interaction with the negatively charged alginate chains. The very first attempt to load B7-005 on Alg/HAp scaffolds was performed by soaking them in an aqueous solution of peptide at increasing concentration, in order to easily assess the amount of peptide binding the scaffold inspecting the solution by UV-spectrophotometry. However, the solution containing the peptide turned whitish within one hour, while water only, used to soak control scaffolds control, remained transparent. The whitish colour of the supernatant was directly dependent with the concentration of the peptide in the solution where scaffolds were soaked in (data not shown). It was therefore impossible to properly measure spectrophotometrically the supernatant of the scaffolds.

It has been hypothesised that the whitish colour was due to the binding and aggregation of the peptide with unspecified chemical species released by the scaffold, most probably the residual gluconate still trapped into the structures after the freeze-drying process. It has been therefore necessary to set-up a robust and easy washing protocol to be applied to all the scaffold to be produced for subsequent experiments. A solution of $CaCl_2$ was used to this aim, in order to preserve the Ca^{2+} ions already included into the scaffolds, necessary to maintain its integrity after re-hydration. To assess the efficacy of a series of washings, scaffolds were washed with $CaCl_2$ until the absorbance of the supernatant was no more significant, indicating that the release of undesired chemicals from the scaffold was ended. The wavelengths of 214 nm and 280 nm were chosen as they represent the gold-standard for the direct UV-quantification of peptides in solution. Therefore, it was of interest to understand if any interference could occur with the quantifying of B7-005 in the supernatant of the scaffolds. Moreover, the wavelengths of 230 nm and 240 were chosen as intermediate, to roughly spot the presence of any other contaminant whose absorbance peak(s) fell in between of the wavelengths used for the quantification of peptides. The washing with $CaCl_2$ was efficient in removing all the undesired chemical species (Figure 4). The protocol was then refined halving the duration and doubling the number of washings. This made the protocol less time consuming and removed even better the last traces of contaminants detectable by UV spectrophotometry (data not shown).

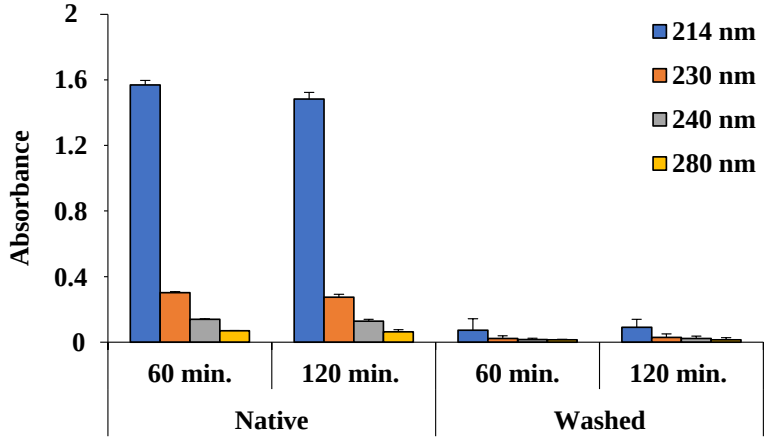

Figure 4. Absorbance reduction at different wavelengths after washing the Alg/HAp scaffolds with $CaCl_2$. Error bars represent the standard deviation calculated on the average of 3 scaffolds.

Once identified the protocol to wash the scaffold, their loading with the B7-005 was repeated. To this aim, the scaffolds were soaked in an aqueous solution of peptide, and again the absorbance of the supernatant was assessed over time in the UV range. A clear time-dependent decrease of the absorbance was observed up to background levels, indicating the progressive and complete adsorption of the peptide on the scaffolds (Figure 5).

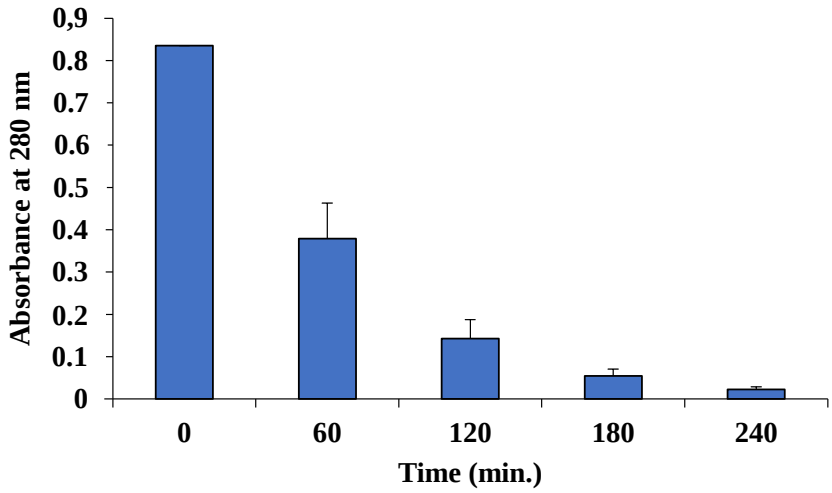

Figure 5. Variation over time of the absorbance of the B7-005 solution used to soak Alg/HAp scaffolds. Error bars represent the standard deviation calculated on the average of 6 scaffolds tested during 2 independent experiments (n=6).

As a function of the measured absorbance of the supernatant, and knowing the initial input of peptide, it has been possible to calculate the amount of peptide loaded on the scaffold. It reached a maximum within 4 hours (Figure 6A), when approximately 100% of the peptide previously in solution was adsorbed on the porous structure. It has then calculated that approximately 9 µg of B7-005 were loaded for each mg scaffold (Figure 6B).

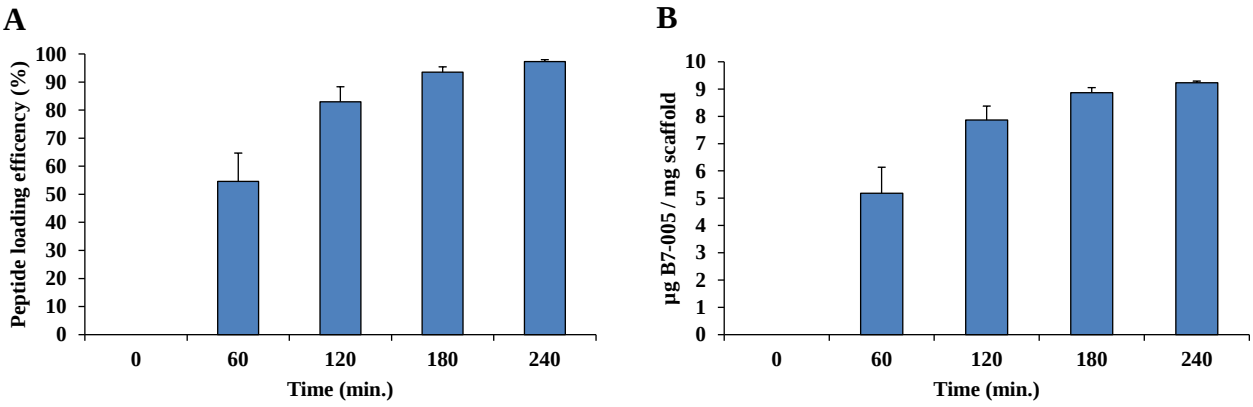

Figure 6. Loading of B7-005 on Alg/HAp scaffolds. A) Percentage of the peptide loaded on the scaffold. B) Loading of µg B7-005/ mg of scaffold. Error bars represent the standard deviation calculated on the average of 6 scaffolds tested during 2 independent experiments (n=6).

Release of B7-005 from Alg/HAp scaffolds

To assess the release of B7-005 from Alg/HAp scaffolds, peptide-loaded scaffolds were soaked in PBS and incubated at 37°C, then the absorbance of the supernatant was assessed at 280 nm by UV-spectrophotometry to quantify the peptide.

The release of B7-005 under the tested conditions was minimal. Even after 72 hours of incubation the absorbance measured with peptide-loaded scaffolds was comparable to that-one of void scaffolds used as control (Fig. 7A). The peptide was therefore firmly adsorbed on the scaffold. After the 72 hours incubation,

B7-005 was forced out of the scaffold, as a control. To this aim, the scaffolds were incubated for further 2 hours adding NaCl to the supernatant to a final solution of 1 M. The NaCl could displace approximately the 70% of the peptide bound on the scaffolds (Fig. 7B), indicating that the electrostatic interaction between the B7-005 and the alginate was extremely strong, and in this case, detrimental for our purpose.

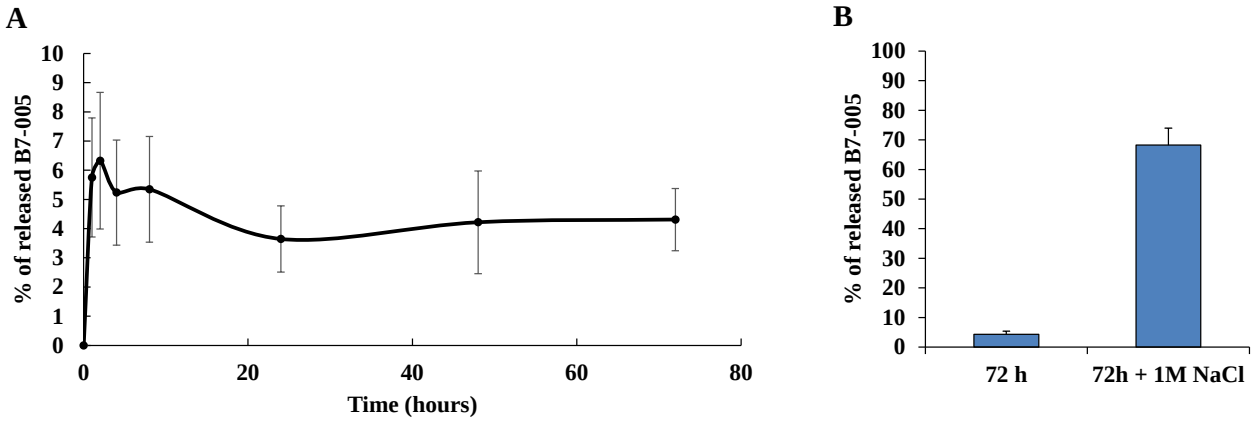

Figure 7. Release of B7-005 from Alg/HAp scaffolds evaluated by UV-absorption of the supernatant. A) The peptides were soaked in PBS at 37°C and the amount of peptide quantified by UV-spec. for 72 hours. B) Release of B7-005 from the scaffolds after the addition of NaCl to 1 M. As a control, scaffolds loaded with water were used to set the blank. Error bars represent the standard deviation calculate on the average of 6 peptide-loaded- and 3 void scaffolds.

A preliminary assay to evaluate if the peptide-loaded scaffold could exert any antimicrobial activity despite the retention of B7-005 on the scaffold surface, was performed soaking the scaffold in a bacterial suspension. Not surprisingly, the peptide-loaded scaffolds in fact did not impair at all the bacterial growth and displayed results basically identical to that of scaffold that received only water instead of peptide (not shown).

Alg/HAp scaffolds coated with lactose-modified chitosan (CTL)

In the attempt to decrease the electrostatic interaction between B7-005 and the alginate, the scaffolds were coated with 0.2% aqueous solution of a positively charged lactose-modified chitosan (CTl, Donati *et al.*, 2005) with the aim to partially saturate their anionic surface. CTL- Alg/HAp coated scaffolds were loaded with the peptide, and non-coated scaffolds were loaded in parallel, as a comparison. The release of B7-005 was then evaluated as reported above. The coating with CTL did not appreciably improve the release of B7-005. The amount of peptide in the supernatant was minimal, so that the measurement was stopped after 48 hours (Figure 8A). A moderate release of peptide (approx. 10%) was assessed after 4 hours of incubation, but unexpectedly it was no more subsequently reported. This could be explained by a re-equilibration of the system after the partial solubilization of the CTL coating, allowing the released fraction of B7-005 to bind back the surface of the scaffold (Figure 8A). As previously, a shock with NaCl was used to displace the peptide still trapped in the scaffold, releasing about 70% of the total payload of B7-005 (Figure 8B). Moreover, the scaffolds after 48 hours were very fragile, their handling started to be very complicated and their integrity was easily compromised. Most probably the repeated freeze-drying cycles and the soaking in CTL may have compromised the structure of the scaffolds.

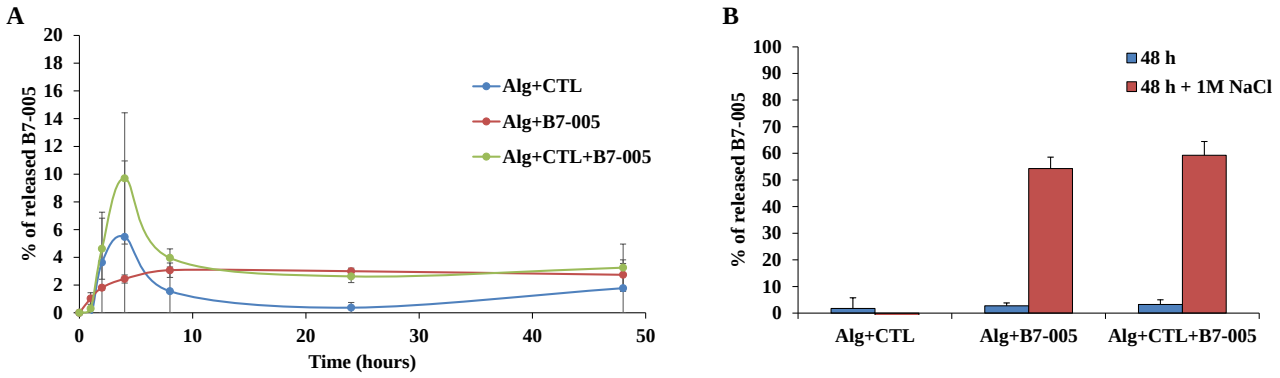

Figure 8. Release of B7-005 from Alg/HAp scaffolds, coated or not with CTL, evaluated by UV-absorption of the supernatant. As a control, scaffolds loaded with water were used to set the blank. A) The peptides were soaked in PBS at 37°C and the amount of peptide quantified by UV-spec. for 48 hours. B) Release of B7-005 from the scaffolds after the addition of NaCl to 1 M. Error bars represent the standard deviation calculated on the average of 3 scaffolds.

Given the inability of the coating to prevent B7-005 sequestration, the protocol was modified increasing the CTL amount to be adsorbed on Alg/HAp scaffolds. The coating was repeated increasing the concentration of the CTL to 1% (w/v). Moreover, the pH of the CTL solution was set at 5.0 in order to confer to CTL more positive charges and help its interaction with the alginate. The loading of B7-005 on the scaffolds was performed as above, however after few hours the supernatant turned whitish, both in the presence and in the absence of peptide (not shown), impairing proper check by UV-spectrophotometry. Probably this was because of the formation of aggregates between the CTL (more abundant than in the previous experiment) and the alginate, maybe made available in solution by the physical stress that the scaffolds underwent during the multiple steps of the protocol. For these multiple problems, considering also the mechanical weakening of the scaffolds due to such a multi-step protocol, the coating of Alg/HAp scaffolds with CTL was abandoned.

Preparation of Agarose 2% / Hydroxyapatite 3% scaffolds

The strong electrostatic interaction between the anionic alginate and the cationic B7-005, although very effective for the loading of the peptide on the scaffold, was detrimental for its release in the environment. The tuning of the surface charge of scaffold with a cationic coating was unsuccessful.

A new strategy was therefore decided in order to overcome the sequestering of B7-005 on the scaffolds. Instead of masking the anionic charge of the polysaccharide composing the scaffold, a different, electrostatically-neutral, polysaccharide was used for their preparation.

Among the many polysaccharides, Agarose (Aga) was a thought to be a valid candidate, since it is electrostatically neutral and it has been already used for the production of scaffolds for the tissue engineering (Chocholata, Kulda and Babuska, 2019).

A new protocol was therefore set up to prepare the scaffolds, substituting the alginate with agarose in the protocol previously used. After proper initial preparatory setting (not shown), porous three-dimensional Agarose 2% / Hydroxyapatite 3% (Aga/HAp) scaffolds were therefore prepared. Their structure was porous, quite homogeneous, and macroscopically comparable with that of Alg/HAp scaffolds used for all the previous experimentation (Figure 9). Aga/HAp scaffolds were therefore considered promising and subjected to further characterization.

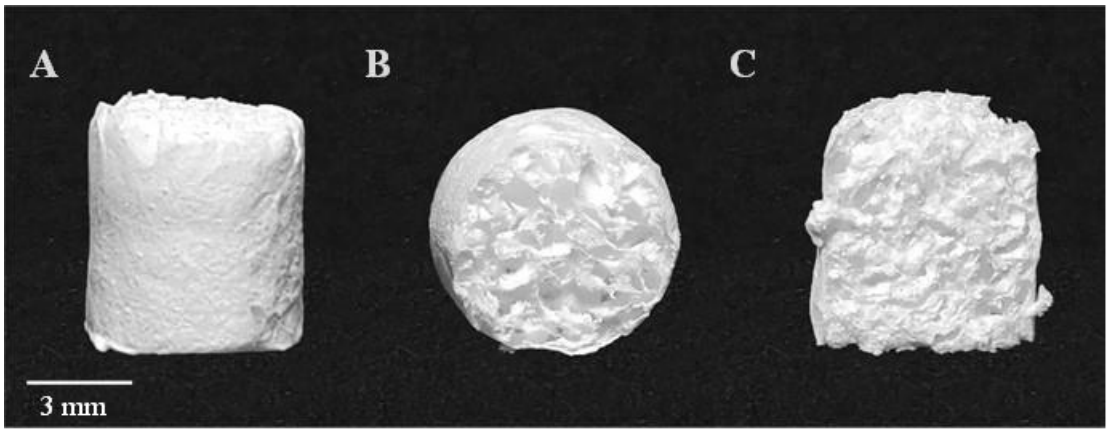

Figure 9. Agarose 2% / Hydroxyapatite 3% scaffolds. The scaffolds were prepared in the wells of a 48-wells plate, then cut to the standard height of 5 mm. A) Frontal view, B) upper view, C) vertical section.

Scanning electron microscopy of Aga/HAp scaffolds

To investigate the structure of Aga/HAp scaffolds at microscopic level, the scaffolds were observed using scanning electron microscopy (SEM). Alg/HAp scaffolds were used as a comparison. The scaffold obtained after substitution of the alginate with the agarose maintained a general aspect, at the microscopic level, similar to that of the original scaffolds composed by alginate. The observations, performed at different magnifications, demonstrated that Aga/HAp scaffolds were porous, their cavities looked interconnected even though the structure on the whole looked quite cavernous (Figure 10 ABC) if compared with that of Alg/HAp scaffolds, which was more lamellar and lofty (Figure 10 DEF).

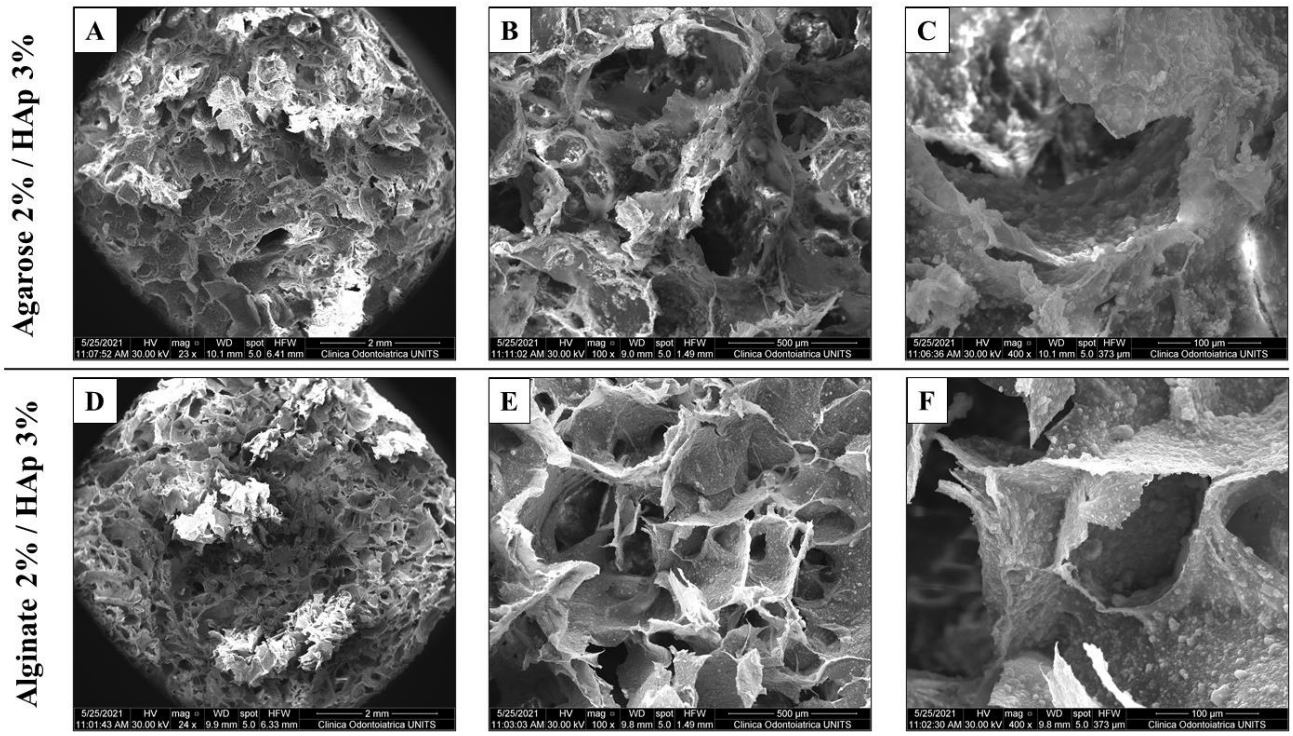

Figure 10. Scanning electron microscopy of Aga/HAp (A,B,C) and Alg/HAp (D,E,F) scaffolds taken at different magnification (24× A,D; 100× B,E; 400× D,F).

Micro-computed tomography on Aga/HAp scaffolds

Once assessed the microstructure of Aga/HAp scaffolds and the similitudes with Alg/HAp scaffolds, further studies were conducted to have more detailed three-dimensional structural data on them. To this aim, micro-computed tomography of Aga/HAp scaffolds was performed, using in parallel Alg/HAp scaffolds as a comparison. Parameters of Aga/HAp scaffolds, such as the total porosity of the structures (≈72%), the average dimension of the pores (≈294 μm) and the average thickness of the trabecula (≈81 μm) (Table 3) were in the range suggested for scaffolds devoted to guided bone regeneration (Bružauskaitė *et al.*, 2016). These parameters were also similar with those determined for Alg/HAp scaffolds. The moderate difference in the anisotropy values between Aga/HAp and Alg/HAp scaffolds (0.45 *vs* 0.53, respectively) (Table 4) may be explained with the different shape of the cavities, that is mainly rounded Aga/HAp and prevalently flattened in Alg/HAp. Results therefore confirmed the similarity between the microstructure of both the types of scaffolds already observed by SEM (Figure 10) and that can be appreciated also looking at the three-dimensional rendering of the samples (Figure 11).

Table 4. Analysis of Aga/HAp and Alg/HAp microstructure by microcomputed tomography.

	Porosity (%)	Trabecular thickness (μm)	Trabecular spacing (μm)	Degree of anisotropy (DA)
Aga/HAp	72.7 ± 2.4	81.2 ± 11.3	294.0 ± 37.6	0.4 ± 0.1
Alg/HAp	79.2 ± 4.6	64.1 ± 8.5	313.1 ± 36.3	0.5 ± 0.1

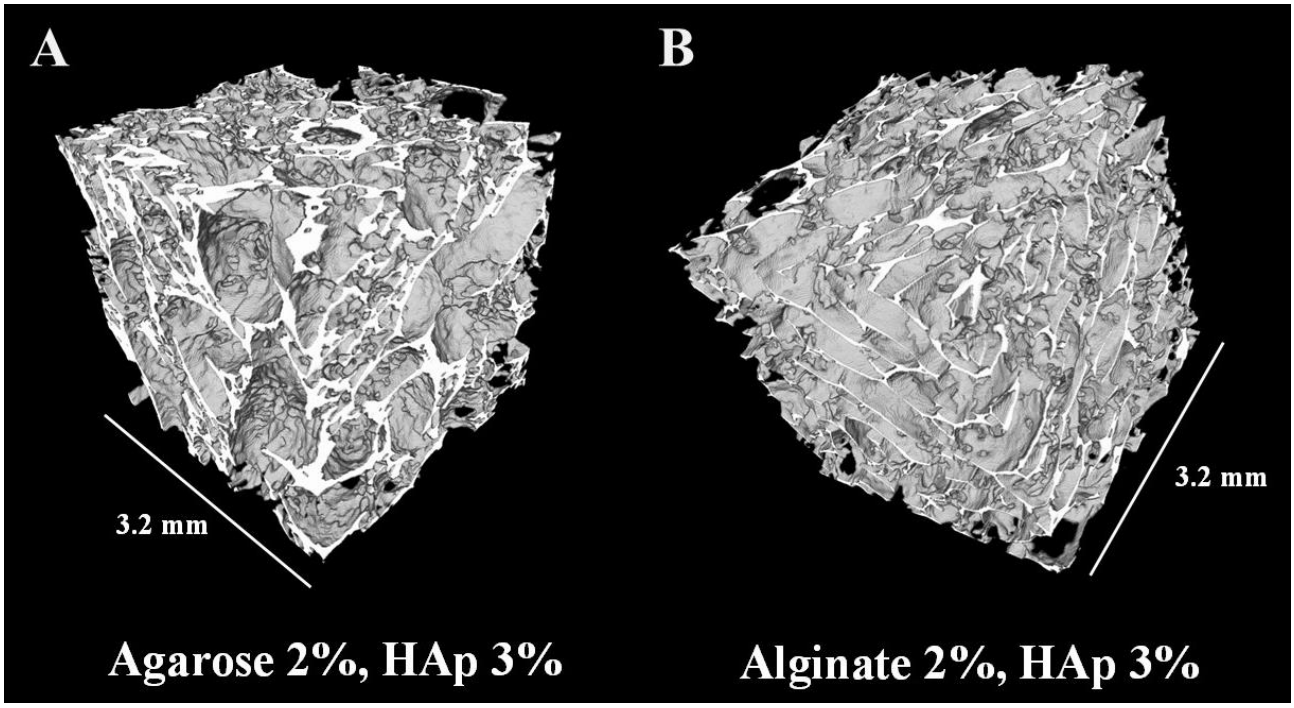

Figure 11. Three-dimensional rendering of Aga/HAp (A) and Alg/HAp (B) scaffolds after micro-computed tomography analysis.

Loading and release of B7-005 with Aga/HAp scaffolds

Given the neutral charge of agarose, the electrostatic adsorption of B7-005 on Aga/HAp scaffold was not possible. Therefore, the scaffolds were soaked in the minimum volume of aqueous B7-005 solution required to homogeneously permeate the structure. The peptide-loaded scaffolds were then freeze-dried to physically trap B7-005 on them. The loading was performed with approximatively 6 μg of B7-005 / mg of scaffold.

The release of peptide from Aga/HAp scaffold was assessed in PBS at 37°C using UV-spectrophotometry. The 70% of the B7-005 input was efficiently and quickly released already after 1 hour. The release continued but was evidently slowed down for the following 3 hours and was almost complete after 24 hours of incubation (Figure 12). Aga/HAp scaffolds therefore did not sequester the peptide and were therefore suitable for the combined use with B7-005. The new formulation with agarose was therefore preferable for antimicrobial destinations compared to the previous-one based on alginate.

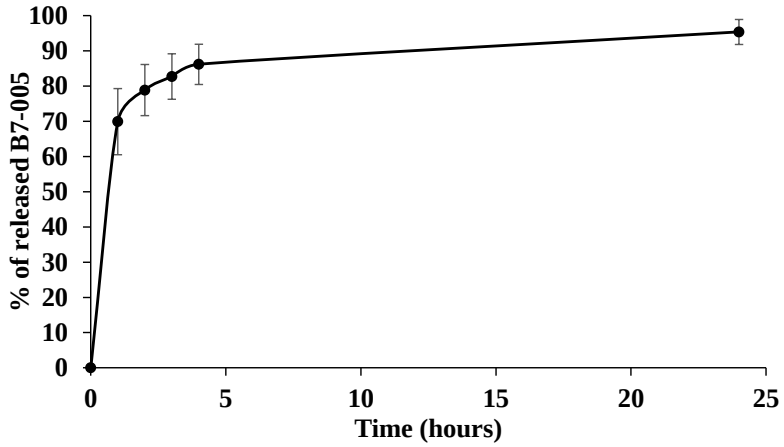

Figure 12. Release of B7-005 in PBS at 37°C from Aga/HAp scaffolds evaluated by UV-absorption of the supernatant. Scaffolds loaded with water only were used to set the blank. Error bars represent the standard deviation calculated on the average of 3 scaffolds.

Proliferation of MG-63 cells on Aga/HAp scaffolds

The compatibility between Aga/HAp scaffolds and the PrAMP B7-005 made them desirable as substitutes for Alg/HAp scaffolds, however there was still no evidence that the new structures could sustain the cell proliferation. To this aim, MG-63 cells were seeded on the Aga/HAp scaffolds and their proliferation was evaluated overtime by Alamar blue assay.

A first setting had been necessary (not shown) to identify an appropriate number of cells to be seeded on the scaffolds, in order to have good signals already in the first time-point of sampling, allowing at the same time the appreciation of the cell proliferation avoiding the premature reaching of a plateau.

Once identified valid experimental conditions, MG-63 cells were seeded on each Aga/HAp scaffold, and their proliferation was assessed for 28 days. Since it was the first evaluation of the efficacy of Aga/HAp to host and sustain a cell population, the experiments focused only on scaffold without the B7-005, in order to avoid multiple factors that could contemporarily affect the cell proliferation.

MG-63 cells could proliferate on the scaffolds. The cell viability reached a maximum after one week of incubation and remained then similar for the following 3 weeks, indicating that the proliferation stopped but also that there was no cell death. The cell proliferation rate was calculated accordingly, and it was estimated that cells quadruplicated their number within the first 7 days (Figure 13). Aga/HAp scaffolds were then suitable for hosting cells and were considered further promising for tissue engineering.

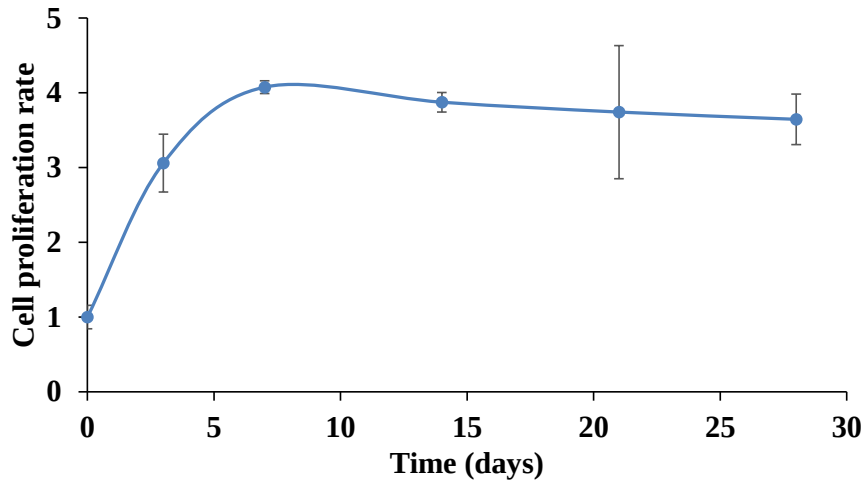

Figure 13. Cell proliferation on Aga/HAp scaffolds assessed by Alamar blue assay. 32000 cells were seeded on each scaffold, and the fluorescence of their supernatant was assessed up to 28 days in order to calculate their proliferation rate. Error bars represent the standard deviation calculated on the average of 3 scaffolds (n=3),

Once assessed the sustainability of a MG-63 cell culture on Aga/HAp scaffolds, in order to evaluate if B7-005 could have hampered the cells proliferation in the scaffolds, the experiment was repeated testing in parallel also scaffolds loaded with B7-005. The same amounts of cells were seeded on scaffolds containing or not the peptide. The viability of the cells population was then assessed for two weeks, a time hypothesised to be sufficient for MG-63 cells to reach the plateau also in the presence of a putative delay due to toxic effect of the peptide.

The cells proliferated both in the presence and in the absence of B7-005, although there was a reduction of the signal within the first week in the presence of peptide. This is likely due to the stressing effect of the quick and massive release of B7-005 from the scaffold. The observed shift may indicate a general reduction of the cells metabolism, or a reduction of the initial cells inoculum due to toxic effects. However, B7-005 did not impair but simply retarded the proliferation of cells, since after two weeks also cells growing on the peptide-treated scaffolds reached similar levels of tshose growing on untreated scaffolds (Figure. 14).

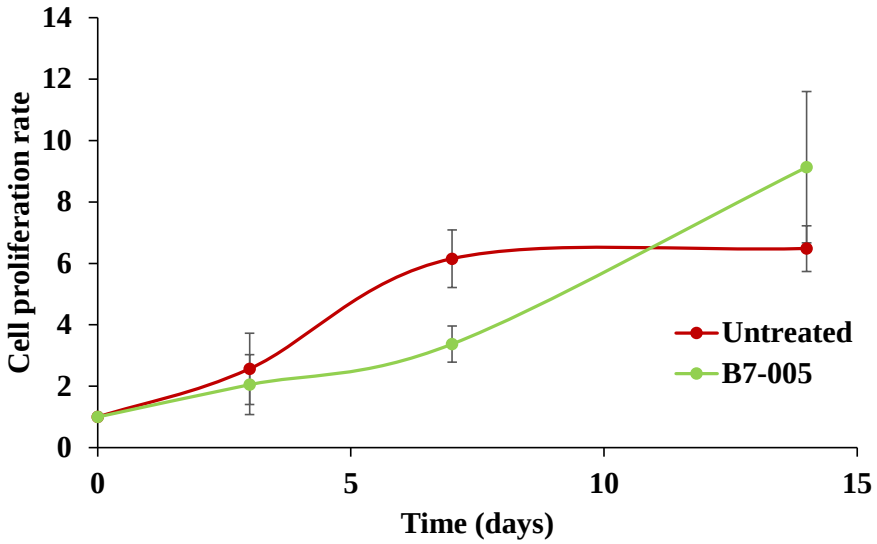

Figure 14. Cells proliferation on Aga/HAp scaffolds assessed by Alamar blue assay in the presence (B7-005) or in the absence (Untreated) of the peptide B7-005. 32000 cells were seeded on each scaffold, and the fluorescence of their supernatant was assessed up to 14 days to calculate the cells proliferation rate. Error bars represent the standard deviation calculated on the average of 3 scaffolds (n=3).

Swelling of Aga/HAp scaffold

After the suitability of Aga/HAp scaffolds (loaded or not with B7-005) for guided bone regeneration was assessed, their deeper morphological and mechanical characterization was needed. In order to investigate their swelling properties, Aga/HAp scaffolds were submerged in phosphate-buffered saline (PBS), then their gain of weight was assessed overtime. The excess of medium was removed from the scaffold, limiting therefore the measurement to the fluid strictly associated with the porous scaffolds. A quick and relevant gain of weight was measured already after 10 minutes, however no further increasing were observed over time up to 4 hours (Figure 15). The swelling test was then prolonged to 24 hours, but no significant changes were reported with respect to the time-point at 4 hours. This is compatible with the rapid permeation of the scaffolds by the PBS, and indicates that the structure of the scaffolds is stable, suggesting that the trabecula remained compact and pointing out that the polymer remained unsolved by the aqueous environment.

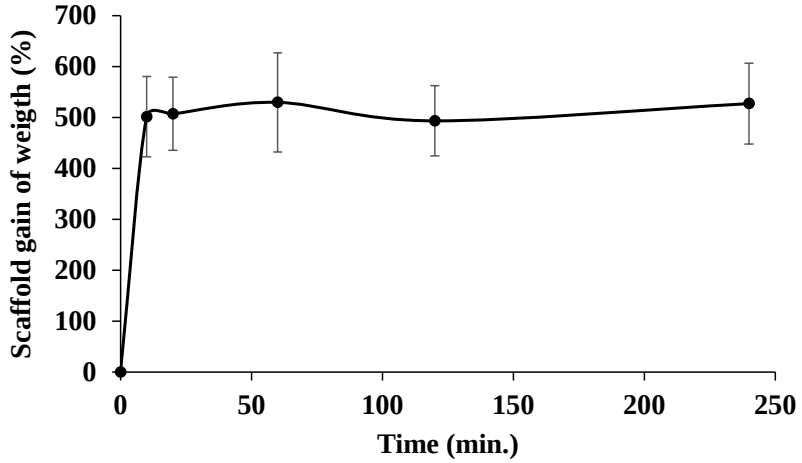

Figure 15. Swelling test of Aga/HAp scaffolds measured as weight increase after incubation in PBS at 37°C. The excess of PBS was removed limiting the study to the fluid strictly associated with the scaffolds. The gain of weight of each scaffold is compared with its dry weight. Error bars indicate the standard deviation calculated on the average of 8 scaffolds (n=8).

Mechanical characterization of Aga/HAp scaffolds

In order to characterize the mechanical properties of Aga/HAp scaffolds, mechanical compression tests were performed on scaffolds in both dry and wet state to obtain stress-strain curves. The elastic modulus (E), the stress value at which the sample reaches the 50% of deformation [50% strain], and the toughness of the biomaterial, were therefore calculated. Taken together mechanical data indicated (in line with what already observed for the Alg/HAp system) that these scaffolds cannot be used for load-bearing applications. Indeed, especially in wet environment, they lose almost any mechanical resistance (Table 5). Therefore, the application of Aga/HAp scaffolds should be limited to the void-filling of the bone defect and to the bridging activity for the cells of the host.

Table 5. Compression tests on dry and wet Aga/HAp scaffolds. Elastic modulus, stress value for 50% deformation and toughness.

	Dry	**Wet**
Elastic modulus (E) (kPa)	38.27 ± 35.35	0.35 ± 0.14
$Stress_{[50\% strain]}$ (kPa)	818.08 ± 279.05	24.59 ± 11.53
Toughness (kJ/mm^3)	23.80 ± 10.45	0.55 ± 0.20

Stability of Aga/HAp scaffolds

Swelling experiments suggested that the structure of Aga/HAp scaffolds remained unchanged for short times in wet environment. To investigate then their stability after long exposure to conditions similar to the physiologic environment, the scaffolds were incubated in simulated body fluid (SBF). At each timepoint, weight variation of scaffolds was evaluated, as the results of degradation (loss of weight) or as the consequence of precipitation of inorganic matrix nucleated by the hydroxyapatite already present in the scaffolds. No loss of weight was observed even after 8 weeks of incubation (Figure. 16). On the contrary a constant gain of weight was evidenced up to +20% after 8 weeks (Figure. 16), most probably explainable with the precipitation of insoluble salts on the scaffolds.

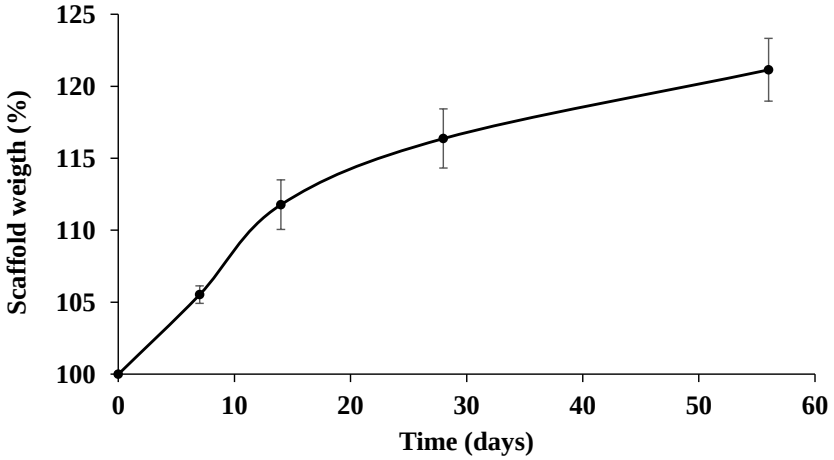

Figure 16. Stability test performed on Aga/HAp scaffolds in SBF at 37°C performed evaluating weight variations before and after the incubation expressed as percentage. Error bars indicate the standard deviation calculated on the average of 4 scaffolds.

Antimicrobial effect of B7-005-loaded Aga/HAp scaffolds toward ESKAPE pathogen

In order to evaluate the efficacy of Aga/HAp scaffolds loaded with the B7-005 peptide to prevent surgical infections, their antimicrobial effect was tested against representative reference strains of clinically relevant pathogens. Bacterial cultures were grown in liquid medium in the presence of Aga/HAp scaffolds loaded or not with the B7-005 peptide. The ability of scaffolds to prevent bacterial proliferation was evaluated measuring

the turbidity of the medium. The lower the absorbance of the medium at 600 nm, the lower the bacterial growth, then the stronger was the antimicrobial effect.

Peptide-loaded scaffolds strongly inhibited the growth of *E. coli*, *K. pneumoniae* and *A. baumannii*. On the other hand, the antimicrobial effect toward *S. aureus* and *P. aeruginosa* was scarce (Figure 17). The scaffolds were therefore endowed with antimicrobial activity, they efficaciously prevented the growth of many clinically relevant pathogens, however their antimicrobial effect did not cover the entire panel of tested microorganisms.

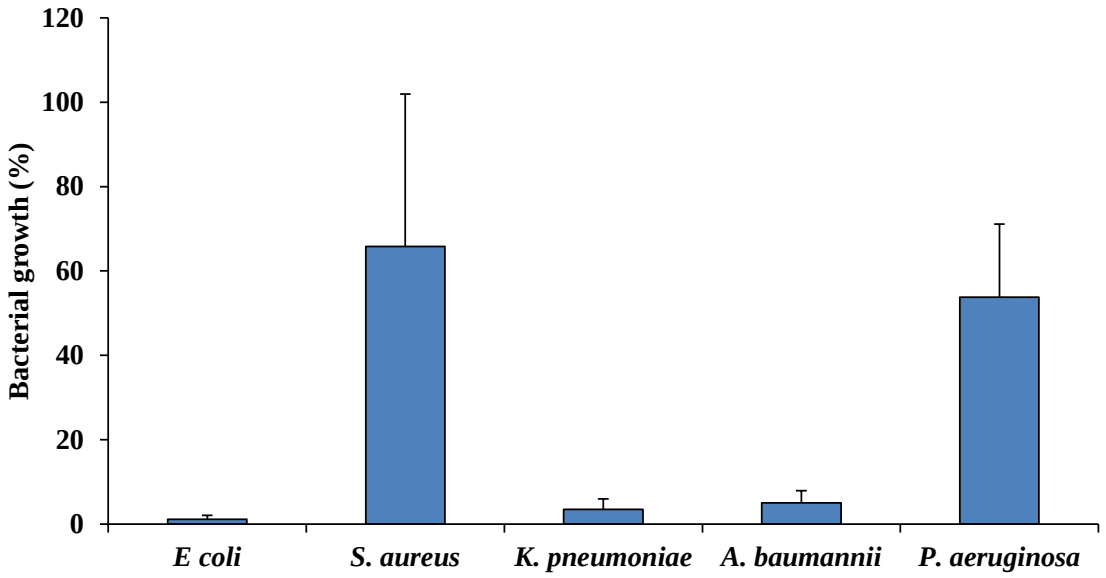

Figure 17. Antimicrobial effect of B7-005-loaed Aga/HAp scaffolds assessed evaluating their capability to prevent bacterial growth in liquid medium, measured by absorbance at 600 nm. Results are expressed as a percentage of identical bacterial cultures growing in the presence of untreated Aga/HAp scaffolds and are the average of two independent experiments (n=2).

Discussion

Aim of this project was to endow alginate/hydroxyapatite scaffolds for bone regeneration with antibacterial activity by the use of an antimicrobial peptide.

As first work package, some efforts were put in enhancing the antibacterial activity of the PrAMP Bac7(1-16). One of the primary problems that were addressed was to encompass in the spectrum of action of this compound pathogens like *S. aureus* and *P. aeruginosa*, that are of serious concern for post-implant bacterial osteomyelitis (Zimmerli and Sendi, 2017). The first selected approach was to systematically modify the sequence of Bac7(1-16) looking for compounds displaying better *per se* antimicrobial effect or broader range of activity. This approach was selected since it was previously successfully used for the modification of another mammalian PrAMP, Bac5(1-17), obtaining derivatives whose antimicrobial activity was significantly ameliorated (Mardirossian *et al.*, 2019). At the end of this optimization process, new Bac7(1-16) derivatives were obtained and characterized, and among them, B7-005 was the most promising. B7-005 in fact retained the efficacy of the native Bac7(1-16) toward pathogens like e.g. *E. coli* and *K, pneumoniae* and displayed improved efficacy in targeting other pathogens like *A. baumanni, P. aeruginosa*, and most interestingly, *S. aureus* (Mardirossian *et al.*, 2020). B7-005 was very well tolerated by human cells, and in the current work, the osteosarcoma cell line MG-63 was selected as a first approximation of the type of cells that the peptide may encounter in the surrounding bony environment immediately after its quick release from the scaffold. Also in this case, B7-005 displayed promising biocompatibility and, although MG-63 represent only a first rough model, the peptide should not damage surrounding bone cells after its release (Figure 2).

Subsequently, in the attempt to further boost the antimicrobial effect of B7-005 toward Gram-positive bacteria, the peptide was converted into a lipopeptide. This process was already shown to improve the antimicrobial effect of antimicrobial peptides (also PrAMPs), especially toward Gram-positive pathogens (Armas *et al.*, 2019, 2021). It could be argued that the binding of the lipid chain to the C-terminus instead of to the N-terminus would have been more respectful for the mode of action proposed for B7-005, that impairs the protein synthesis most probably binding the ribosomal exit tunnel (Mardirossian *et al.*, 2020). However, the lipidation performed on Bac7(1-16) by Armas et al. pushed the mode of action of the lipopeptide toward the permeabilization of the bacterial membrane. This suggested that the activity on the ribosome, typical of Bac7(1-16) was therefore lost or at least reduced (Armas *et al.*, 2021). As a consequence, considering that lipidation would have pushed B7-005 toward a fully permeabilizing mode of action, it has been decided to link the fatty chain to the N-terminus, regardless of the importance of the N-terminus for the activity of several PrAMPs (Graf *et al.*, 2017; Mardirossian *et al.*, 2018). This answered mainly the technical need for a simpler synthesis, as the linking of the fatty chain on the N-terminus was compatible with solid-phase synthesis on resin, and it was therefore easier and less expensive than a C-terminal lipidation. In hindsight, one may think that it would have been better to link the lipid moiety to the C-terminus, since the N-terminal lipidation was in the end detrimental for the activity of B7-005. Indeed, unlike the expectation, there were no benefits toward *S. aureus*, and the procedure was even worsened with respect to the activity of the lipopeptide toward *E. coli* (Table 3). On the other hand, the lipidation of B7-005 decreased its biocompatibility, making it more aggressive toward the human osteosarcoma cell line MG-63 (Figure 3). The marked permeabilization identified in cells treated with the lipopeptide, together with its lipidic moiety, suggest that the membrane destabilization may be the cause of the cytotoxicity of lipoB7-005. Anyhow, cell permeabilization has been observed after 24 hours of incubation, when it was no more possible to discriminate if the membrane permeabilization was the cause or the consequence of the cell death (Figure 3). So, the aggression of eukaryotic membranes by lipoB7-005 is reasonable, but it must be limited to an hypothesis. Further studies would have been desirable to define the effect of C-terminal lipidation of B7-005 on its antimicrobial or cytotoxic mechanism, however this analysis was out of the topic of this project, and the lipoB7-005 was abandoned. Only B7-005 in the end was maintained to be loaded on the scaffolds.

The loading of the peptide on the scaffolds has not been so obvious and required a minimum of setting up in order to be optimized. Usually, Alg/HAp scaffolds were most commonly used in their re-hydrated form mainly for cell proliferation assays. Commonly, these protocols involved a first step consisting in conditioning the

scaffolds with cell growth medium, before seeding any cell population. This step, other than hydrating scaffolds and soaking them with proper nutrients for cells, provides also a washing of these structures, removing any left-over of undesired reagents of the gelling process still trapped into the scaffolds after lyophilization. However, the need to load the antimicrobial peptide as preliminary step before any other biological test, and also before the conditioning step, unmasked the problem to remove these undesired leftovers. It has been necessary therefore to set up a washing protocol before starting the loading of B7-005 on the scaffolds (Figure 4). A $CaCl_2$ solution was used to wash the scaffolds, in order to prevent Ca^{2+} pauperization that would have affected their integrity, destabilizing the egg-box structures crosslinking the alginate chains (Cao *et al.*, 2020). Most probably, the chemical species that impaired the first attempts to load B7-005 on scaffold were the gluconic acid and residual not crosslinked alginate (maybe short chain fragments) released by the trabecula. Both these anionic compounds may have complexed the peptide or may have reduced its solubility, explaining therefore why the aqueous solution of peptide turned whitish after the incubation with unwashed Alg/HAp scaffolds.

Once removed any interfering compound, the electrostatic adsorption of B7-005 on the scaffolds was very efficient, since almost all the peptide was loaded after 3 hours, and the adsorption was basically 100% of the initial payload after four hours (Figures 5 and 6). However, if the strong interaction between the anionic alginate and the arginines of B7-005 was excellent in promoting the binding of the peptide on the scaffold, on the other hand it was excessively tenacious to allow the release of the compound under physiological conditions (Figure 7). To the best of our knowledge, PrAMPs and their derivatives need to be free in solution in order to perform their antimicrobial activity. Unlike other AMPs, PrAMPs are therefore not promising candidates for permanent surface derivatization since they need to be released into the environment to target bacteria. This was the case also of B7-005, whose biological activity was hampered by the retention on the alginate matrix. In fact, Alg/HAp scaffolds loaded with the peptide displayed no antimicrobial effect at all, as evaluated during preliminary antimicrobial activity assays (not shown). Alginate-based scaffold therefore are not appropriate for loading with AMPs, neither looking at the possibility to have the peptide slowly released during the scaffold degradation. Most probably, the peptide would in fact remain firmly attached to the alginate chains that detach from the scaffolds during its decomposition. Also in this case however it could not exert any antibacterial effect. It has to be said that there is no clear indication of the inopportunity to combine alginate and antimicrobial peptides in literature. Compared to the remarkable amount of papers on alginate-based scaffolds or on antimicrobial peptides, Scopus provides only 69 papers using as query “antimicrobial AND peptide AND alginate”. This lack of published papers may be due to the same problems reported also in the current work, that prevented the publication of high-impact data or that induced authors to follow different protocols in preparing their systems. From one point of view, the interaction of alginate with antimicrobial peptides (and also its inactivating properties) are well documented, *e.g.* bacterial alginate represents one of the factors explaining the resistance of some strains of *Pseudomonas aeruginosa* to AMPs (Chan, Burrows and Deber, 2004) (Chan, Burrows and Deber, 2005). On the other hand, alginate-based structures have been tested in combination with AMPs, suggesting that, in principle, it was possible to modulate this interaction and to exploit the binding between AMPs and alginate for research purposes. Topazzini and colleagues demonstrated that the release of the AMP LL-37 included in gel beads composed by 2% Alginate and 3% Hydroxyapatite was very slow, but still evident. Moreover, they showed that the peptide maintained its antimicrobial activity in the presence of a small amount of soluble alginate (in the presence of diluted growth medium). However, looking at the results *ex post*, authors did not test nor discuss the antimicrobial activity of the beads loaded with LL-37 (Toppazzini *et al.*, 2011). There is no indication therefore if this aspect was not investigated, or if it has been, but the results were considered unsatisfactory and not published. To further complicate the system, it has to be considered that the transfer of these results from LL-37 to B7-005 was not obvious. LL-37 is an alpha-helical antimicrobial peptide, that is moreover prone to oligomerisation, (Xhindoli *et al.*, 2016), while B7-005 is believed to be linear, according to its composition and the presence of 3 prolines out of 16 total residues (Mardirossian *et al.*, 2020). The interactions observed by Topazzini and colleagues therefore may have been influenced also by the secondary structure of the peptide, and not be completely due to the electrostatic interactions. In a more recent work an antimicrobial peptide was successfully released from an alginate structure (although jelly) still displaying a pale but observable antimicrobial effect (Mateescu *et al.*,

2015). It was then reported that a short Arg/Trp rich peptide displayed slow but constant release of from an alginate-based matrix retaining impressive antimicrobial activity (although the measurement of this effect was no clearly described in the paper) (Lin *et al.*, 2019). It was therefore worth to try the loading of B7-005 on the scaffold, as its behaviour would have been not obvious. Moreover, at the beginning of this project, it has been hypothesised that in case of block of B7-005 by alginate, there would have been still possibility to modulate this interaction. Previous evidences described problematic retention of peptides (although not antimicrobial) in alginate matrices, that was reduced by decreasing the overall charge of the matrix (Mumper *et al.*, 1994). Overall, data about the combined use of alginate and AMPs are often discording but were in the end somehow encouraging. However, the results obtained in the present work would discourage the use AMPs on alginate-derived structures. The dissemination of the difficulties encountered in preparing systems combining alginate and antimicrobial peptide would be desirable, as well as it would be a critical analysis and review of the evidences reported in literature.

Also the attempts to partially mask the strong negative surface charge of the scaffolds using a positively charged polymer (lactose-modified chitosan, CTL) did not bring significant improvements in releasing the peptide, unlike a similar approach described by (Mumper *et al.*, 1994) using different polymers but the same rationale. Given the ineffectiveness of the soaking of the scaffold with the 0.2% (w/v) solution of CTL in affecting both peptide loading and release, it is evident that the residual surface charge of the scaffold was more than sufficient to sequester B7-005 (Figure 8). The increase of the amount of CTL, and the reduction of the pH during the coating (to increase the CTL positive charge) was neither decisive, since the big amount of cationic polymer started to be detrimental, and even affected technically the loading of the peptide.

Moreover, the complete protocol for preparing Alg/HAp scaffold, considering the washings, the sterilization step, potentially any coating, and lastly the loading with the peptide, became a multi-step protocol including several wetting/freeze-drying cycles. All these procedures started to affect heavily the integrity of the porous structure of scaffolds. These considerations suggested that the use of alginate may have not been the best direction to follow in order to prepare three-dimensional polysaccharide scaffolds to be loaded with antimicrobial peptides.

Considering that the insurmountable problem (at least within the temporal horizon of this project) encountered using Alg/HAp scaffolds was their negative electrostatic charge, it has been decided to prepare scaffolds starting from an electrostatically neutral polysaccharide. This approach seemed simpler than spending energies in masking partially the problematic negative charge of the alginate. Agarose is easy to handle and not excessively expensive, its polymerization is rapid and simple, and the compound is stable and safe. For these reasons, agarose had been already used for tissue-engineering purposes (Chocholata, Kulda and Babuska, 2019), although there is not the strong background characterizing the use of alginate, chitosan or other biopolymers. Among the applications, agarose (although in its gel form) has already been used in combination with hydroxyapatite to promote the regeneration of osteochondral defects (Khanarian *et al.*, 2012). First attempts have been made to obtain three-dimensional porous scaffolds. Agarose was mixed with hydroxyapatite (alone or in combination with *e.g.* calcium triphosphate) to cast some gels that once freeze-dried provided porous scaffolds suitable to promote the regeneration of bone tissue. (Sánchez-Salcedo, Nieto and Vallet-Regí, 2008) (Peña *et al.*, 2010) (Román *et al.*, 2011). Interestingly, the proportion amount of polysaccharide and ceramic compounds used for these structures described in literature were not so far from those indicated by our protocols to prepare Alg/HAp scaffolds. Moreover, similar porous scaffolds composed by agarose and hydroxyapatite were prepared aiming not only at tissue regeneration but also at the release of drugs in the site of grafting, and the biocompatibility of these structures was assessed with cell lines approximating the bone tissue (Paris *et al.*, 2015; Witzler *et al.*, 2019). Agarose was therefore considered suitable for the aim of this project, and the protocol previously used to prepare Alg/HAp scaffolds was modified substituting alginate with agarose.

Aga/HAp scaffolds were successfully prepared in the current work adapting the protocol previously described for the Alg/HAp system by Turco and colleagues (Turco *et al.*, 2009). Three-dimensional porous scaffolds were obtained, and after macro-and microscopical inspection, their aspect, structure and porosity resulted

similar not only to that of Alg/HAp, but also to other agar-based scaffold reported in literature (Figure 10 and 11) (Turco *et al.*, 2009; Román *et al.*, 2011; Paris *et al.*, 2015; Witzler *et al.*, 2019). The more complex analysis following the micro-computed tomography of Aga/HAp scaffolds, confirmed their similarity with the other scaffolds reported above, but also indicated that the pores dimension and the overall porosity of the structures was suitable for promoting the growth of bone tissue (Bružauskaitė *et al.*, 2016).

The loading of B7-005 on Aga/HAp needed not surprisingly a change of protocol with respect to Alg/HAp scaffold. The soaking of the scaffolds with concentred peptide solution and their following freeze-drying was effective and simple, therefore it was adopted as standard protocol. The release of the B7-005 from the scaffold was rapid and massive, and reached the totality after 24 hours (Figure 12), in line with what reported in literature using quite similar agarose-based scaffold loaded with other drugs (Paris *et al.*, 2015; Witzler *et al.*, 2019). As first, the possibility to efficiently load and release the peptide represented an evident advantage of the use of agarose instead of alginate. Moreover, the rapid release of peptide from the scaffold fits well with the intended future medical practice. Considering that the highest risk of infection associated to bone-grafting takes place during the implant, a quick and massive release of the peptide may inactivate quickly any pathogen, before the onset of any infection. On the other hand, this very fast release of B7-005 may expose the peptide to the risk to be washed away already during the surgical procedure for implant. Moreover, this burst of peptide may exert undesired toxic effect on the host cells. Should be this true, the quick release would be detrimental for an efficient antimicrobial effect of the scaffolds, however, this may be retarded optimizing further coatings for the scaffolds to modulate and retard the release of the peptide. The tuning of the release of the peptide from the scaffolds may become an interesting topic for further studies.

Cell proliferation studies demonstrated that MG-63 cells can adhere and proliferate within the Aga/HAp scaffolds developed in this study. These results are in agreement with previous evidences collected using the same cell line to demonstrate the biocompatibility of agarose-based scaffold (Witzler *et al.*, 2019). The duration of our experiment was prolonged with respect to the assay done by Witzler and colleagues, in order to evaluate not only the viability of cells after exposure to the scaffolds, but also their proliferation on a longer time span (Figure 13). MG-63 cells proliferated vivaciously up to one week but, after that point, a plateau was reached (Figure 13). This indicated that the cells, although remaining viable and healthy, could no furtherly proliferate. A possible explanation of this stop may come from the static conditions used for cell proliferation assays. Considering that scaffolds are porous and three-dimensional, dynamic cell growth condition would probably be preferable (*e.g.* using a bioreactor) instead of static incubation in plate. The flux of growth medium provided by an hypothetical bioreactor may provide more oxygen and nutrients (and the efflux of metabolites) also in the inner part of scaffolds, allowing cells to grow and proliferate also in the core of the structure. Further studies in this direction may allow to enhance the colonization by cell of Aga/HAp scaffolds, and the evaluation of the spatial distribution of cells within the scaffold may also help in optimising the system.

Interestingly, also B7-005 – loaded Aga/HAp scaffolds allowed cells adhesion and proliferation similarly to what untreated scaffolds did, although with a temporal delay, most probably due to the shock that adhering cells had to face for the presence of a high concentration of peptide. Anyhow, once the peptide was removed after 24 hours, simulating the unavoidable clearing that B7-005 would experience *in vivo* (most probably occurring even in shorter time), MG-63 cells could fully recover, reaching the same growth plateau of untreated samples (Figure 14). This was encouraging for the use of the Aga/HAp – B7-005 combined system to promote cells regeneration.

The last point to be tested in the current work was the capability of peptide-loaded scaffold to inhibit the growth of clinically relevant pathogens. To this aim, reference strains of *E. coli, S. aureus, K. pneumoniae, A. baumanni, P. aeruginosa* were used, since most of them are included in the ESKAPE group, that collects some of the most worrisome pathogens displaying marked antibiotic-resistance phenomena (Mulani *et al.*, 2019). The efficacy of B7-005 in preventing the growth of these pathogens had been previously assessed (Mardirossian *et al.*, 2020) and knowing these thresholds, the amount of peptide to be loaded on the scaffolds was decided accordingly, in order to roughly guarantee a B7-005 payload sufficient to inhibit the growth of all of these pathogens once released in a contained volume of solvent. Therefore, an inhibiting effect of B7-005

loaded scaffold was expected toward all the bacterial species used in the experiments. Anyhow, *S. aureus* and *P. aeruginosa* were not significantly affected by the peptide-loaded scaffolds and could unexpectedly grow. On the other hand, the growth of *E. coli K. pneumoniae* and *A. baumanni*, was impaired by the B7-005 loaded structures. This may find an explanation considering that all these three bacterial species express the membrane transporter SbmA or its homologue. B7-005 has been optimized in order to evade the dependency on this membrane protein for its mode of action, however the transporter may anyhow represent a preferential access for the peptide to the bacterial cytosol. To our knowledge, nothing prevents in fact B7-005 from following the ordinary route that is exploited by unmodified PrAMPs to enter bacteria.

The B7-005, tested alone and in solution, displayed an MIC on *S. aureus* and *P. aeruginosa* of 12 µM and 32 µM, respectively, corresponding approximately to 28 µg/mL and 75 µg/mL. The concentration of the B7-005 released by the scaffold under the conditions used for antimicrobial activity test, was expected to be approximately 45 µg/mL after the first hour and 60 µg/mL after 24 hours of incubation (see Figure 12). Theoretically speaking therefore, the amount of peptide released by the scaffold in the supernatant should have been high enough to impair the growth of *S. aureus*, while on the other hand, it was below the MIC for *P. aeruginosa*. However, also *S. aureus* grew in the presence of the B7-005-loaded scaffold, indicating that in spite of the predicted release, the amount of peptide available in the supernatant for antimicrobial activity was lower. This could find explanation in the formation of an equilibrium between the scaffold and the medium components, that made less available the peptide. Otherwise, the peptide could have lost part of its activity because of some interfering components released by the scaffolds whose presence was previously not suspected. In the end, the B7-005 – loaded scaffolds were effective in preventing the growth of pathogenic bacteria, however did not impair the proliferation of some of the pathogens that are of relevant concern for orthopaedic infections, especially *S. aureus*. Further studies will be necessary to understand the reason of this reduction in the antimicrobial activity that scaffold displayed with respect to the expectation. Moreover, once the possibility to use AMPs in combination with the scaffolds prepared in this study has been demonstrated, similar experiments could be repeated using different peptides, more effective toward *S. aureus*, to be loaded on Aga/HAp scaffolds.

CONCLUSIONS

The current work aimed at loading antimicrobial peptides on Alg/HAp scaffolds to help the regeneration of hard tissue defects. The combined use of alginate-derived structures and the antimicrobial peptide B7-005 was not successful, therefore the same protocol used to prepare Alg/HAp scaffolds, with minor adjustments, was successfully adapted to produce Aga/HAp porous scaffolds. These scaffolds where characterized and their 3D-structure as well as their biocompatibility were assessed, demonstrating they are suitable for bone regeneration. The substitution of alginate with agarose made possible the proper loading and releasing of the B7-005 from the scaffolds with kinetics that were described in the results section of the present manuscript. The peptide-loaded scaffolds were compatible with a human cell line and inhibited the growth of some pathogens of clinical relevance. The current work represents a proof of concept that the combined system of antimicrobial peptides and 3D-porous agar-based scaffolds may represent a significant answer to the need to treat bone defect in the age of bacterial antibiotic-resistance.

ACKNOWLEDGEMENTS

I would like to thank the whole research group directed by my supervisor Prof. Gianluca Turco for the support during this project, the whole research group directed by Prof. Donati (University of Trieste) for the availability to share reagents and instruments, and the whole research group directed by of Prof. Scocchi (University of Trieste) for the availability to share the workspace, reagents and instruments.

REFERENCES

Albrektsson T. and Johansson C. (2001) 'Osteoinduction, osteoconduction and osseointegration', *European Spine Journal*, 10(0), pp. S96–S101. doi:10.1007/s005860100282.

Armas, F. *et al.* (2019) 'Design, antimicrobial activity and mechanism of action of Arg-rich ultra-short cationic lipopeptides', *PLOS ONE*. Edited by S. Bhattacharjya, 14(2), p. e0212447. doi:10.1371/journal.pone.0212447.

Armas, F. *et al.* (2021) 'Effects of Lipidation on a Proline-Rich Antibacterial Peptide', *International Journal of Molecular Sciences*, 22(15), p. 7959. doi:10.3390/ijms22157959.

Benincasa, M. *et al.* (2004) 'Antimicrobial activity of Bac7 fragments against drug-resistant clinical isolates', *Peptides*, 25(12), pp. 2055–2061. doi:10.1016/j.peptides.2004.08.004.

Boix-Lemonche, G. *et al.* (2020) 'Covalent grafting of titanium with a cathelicidin peptide produces an osteoblast compatible surface with antistaphylococcal activity', *Colloids and Surfaces B: Biointerfaces*, 185, p. 110586. doi:10.1016/j.colsurfb.2019.110586.

Bormann, N. *et al.* (2017) 'A short artificial antimicrobial peptide shows potential to prevent or treat bone infections', *Scientific Reports*, 7(1), p. 1506. doi:10.1038/s41598-017-01698-0.

Bose, S., Roy, M. and Bandyopadhyay, A. (2012) 'Recent advances in bone tissue engineering scaffolds', *Trends in Biotechnology*, 30(10), pp. 546–554. doi:10.1016/j.tibtech.2012.07.005.

Bružauskaitė, I. *et al.* (2016) 'Scaffolds and cells for tissue regeneration: different scaffold pore sizes—different cell effects', *Cytotechnology*, 68(3), pp. 355–369. doi:10.1007/s10616-015-9895-4.

Cao, L. *et al.* (2020) 'Egg-box model-based gelation of alginate and pectin: A review', *Carbohydrate Polymers*, 242, p. 116389. doi:10.1016/j.carbpol.2020.116389.

Chan, C., Burrows, L.L. and Deber, C.M. (2004) 'Helix Induction in Antimicrobial Peptides by Alginate in Biofilms', *Journal of Biological Chemistry*, 279(37), pp. 38749–38754. doi:10.1074/jbc.M406044200.

Chan, C., Burrows, L.L. and Deber, C.M. (2005) 'Alginate as an auxiliary bacterial membrane: binding of membrane-active peptides by polysaccharides*', *Journal of Peptide Research*, 65(3), pp. 343–351. doi:10.1111/j.1399-3011.2005.00217.x.

Chocholata, P., Kulda, V. and Babuska, V. (2019) 'Fabrication of Scaffolds for Bone-Tissue Regeneration', *Materials*, 12(4), p. 568. doi:10.3390/ma12040568.

Croisier, F. and Jérôme, C. (2013) 'Chitosan-based biomaterials for tissue engineering', *European Polymer Journal*, 49(4), pp. 780–792. doi:10.1016/j.eurpolymj.2012.12.009.

Dimitriou, R. *et al.* (2011) 'Bone regeneration: current concepts and future directions', *BMC Medicine*, 9(1), p. 66. doi:10.1186/1741-7015-9-66.

Domalaon, R. *et al.* (2018) 'Short Proline-Rich Lipopeptide Potentiates Minocycline and Rifampin against Multidrug- and Extensively Drug-Resistant Pseudomonas aeruginosa', *Antimicrobial Agents and Chemotherapy*, 62(4). doi:10.1128/AAC.02374-17.

Donati, I. *et al.* (2005) 'The aggregation of pig articular chondrocyte and synthesis of extracellular matrix by a lactose-modified chitosan', *Biomaterials*, 26(9), pp. 987–998. doi:10.1016/j.biomaterials.2004.04.015.

Einhorn, T.A. and Gerstenfeld, L.C. (2015) 'Fracture healing: mechanisms and interventions', *Nature Reviews Rheumatology*, 11(1), pp. 45–54. doi:10.1038/nrrheum.2014.164.

Fernandez de Grado, G. *et al.* (2018) 'Bone substitutes: a review of their characteristics, clinical use, and perspectives for large bone defects management', *Journal of Tissue Engineering*, 9, p. 204173141877681. doi:10.1177/2041731418776819.

Florin, T. *et al.* (2017) 'An antimicrobial peptide that inhibits translation by trapping release factors on the ribosome', *Nature Structural & Molecular Biology*, 24(9), pp. 752–757. doi:10.1038/nsmb.3439.

Graf, M. *et al.* (2017) 'Proline-rich antimicrobial peptides targeting protein synthesis', *Natural Product Reports*, 34(7), pp. 702–711. doi:10.1039/C7NP00020K.

Inzana, J.A. *et al.* (2016) 'Biomaterials approaches to treating implant-associated osteomyelitis', *Biomaterials*, 81, pp. 58–71. doi:10.1016/j.biomaterials.2015.12.012.

Karageorgiou, V. and Kaplan, D. (2005) 'Porosity of 3D biomaterial scaffolds and osteogenesis', *Biomaterials*, 26(27), pp. 5474–5491. doi:10.1016/j.biomaterials.2005.02.002.

Kazemzadeh-Narbat, M. *et al.* (2010) 'Antimicrobial peptides on calcium phosphate-coated titanium for the prevention of implant-associated infections', *Biomaterials*, 31(36), pp. 9519–9526. doi:10.1016/j.biomaterials.2010.08.035.

Khan, S.N. *et al.* (2005) 'The Biology of Bone Grafting', *Journal of the American Academy of Orthopaedic Surgeons*, 13(1), p. 10.

Khanarian, N.T. *et al.* (2012) 'A functional agarose-hydroxyapatite scaffold for osteochondral interface regeneration', *Biomaterials*, 33(21), pp. 5247–5258. doi:10.1016/j.biomaterials.2012.03.076.

Kokubo, T. and Yamaguchi, S. (2016) 'Novel bioactive materials developed by simulated body fluid evaluation: Surface-modified Ti metal and its alloys', *Acta Biomaterialia*, 44, pp. 16–30. doi:10.1016/j.actbio.2016.08.013.

Krizsan, A., Knappe, D. and Hoffmann, R. (2015) 'Influence of the *yjiL-mdtM* Gene Cluster on the Antibacterial Activity of Proline-Rich Antimicrobial Peptides Overcoming Escherichia coli Resistance Induced by the Missing SbmA Transporter System', *Antimicrobial Agents and Chemotherapy*, 59(10), pp. 5992–5998. doi:10.1128/AAC.01307-15.

Lieberman, J.R. and Friedlaender, G.E. (eds) (2005) *Bone regeneration and repair: biology and clinical applications*. Totowa, N.J: Humana Press.

Lin, H.-R. and Yeh, Y.-J. (2004) 'Porous alginate/hydroxyapatite composite scaffolds for bone tissue engineering: Preparation, characterization, andin vitro studies', *Journal of Biomedical Materials Research*, 71B(1), pp. 52–65. doi:10.1002/jbm.b.30065.

Lin, Z. *et al.* (2019) 'Biofunctions of antimicrobial peptide-conjugated alginate/hyaluronic acid/collagen wound dressings promote wound healing of a mixed-bacteria-infected wound', *International Journal of Biological Macromolecules*, 140, pp. 330–342. doi:10.1016/j.ijbiomac.2019.08.087.

Lindsey, R.W. *et al.* (2006) 'The efficacy of cylindrical titanium mesh cage for the reconstruction of a critical-size canine segmental femoral diaphyseal defect', *Journal of Orthopaedic Research*, 24(7), pp. 1438–1453. doi:10.1002/jor.20154.

Magana, M. *et al.* (2020) 'The value of antimicrobial peptides in the age of resistance', *The Lancet Infectious Diseases*, 20(9), pp. e216–e230. doi:10.1016/S1473-3099(20)30327-3.

Mahlapuu, M. *et al.* (2016) 'Antimicrobial Peptides: An Emerging Category of Therapeutic Agents', *Frontiers in Cellular and Infection Microbiology*, 6. doi:10.3389/fcimb.2016.00194.

Mardirossian, M. *et al.* (2018) 'The Dolphin Proline-Rich Antimicrobial Peptide Tur1A Inhibits Protein Synthesis by Targeting the Bacterial Ribosome', *Cell Chemical Biology*, 25(5), pp. 530-539.e7. doi:10.1016/j.chembiol.2018.02.004.

Mardirossian, M. *et al.* (2019) 'Proline-Rich Peptides with Improved Antimicrobial Activity against *E. coli* , *K. pneumoniae* , and *A. baumannii*', *ChemMedChem*, 14(24), pp. 2025–2033. doi:10.1002/cmdc.201900465.

Mardirossian, M. *et al.* (2020) 'Peptide Inhibitors of Bacterial Protein Synthesis with Broad Spectrum and SbmA-Independent Bactericidal Activity against Clinical Pathogens', *Journal of Medicinal Chemistry*, 63(17), pp. 9590–9602. doi:10.1021/acs.jmedchem.0c00665.

Marsich, E. *et al.* (2013) 'Nano-composite scaffolds for bone tissue engineering containing silver nanoparticles: preparation, characterization and biological properties', *Journal of Materials Science: Materials in Medicine*, 24(7), pp. 1799–1807. doi:10.1007/s10856-013-4923-4.

Mateescu, M. *et al.* (2015) 'Antibacterial Peptide-Based Gel for Prevention of Medical Implanted-Device Infection', *PLOS ONE*. Edited by C. Shih, 10(12), p. e0145143. doi:10.1371/journal.pone.0145143.

Mattiuzzo, M. *et al.* (2007) 'Role of the Escherichia coli SbmA in the antimicrobial activity of proline-rich peptides', *Molecular Microbiology*, 66(1), pp. 151–163. doi:10.1111/j.1365-2958.2007.05903.x.

Mulani, M.S. *et al.* (2019) 'Emerging Strategies to Combat ESKAPE Pathogens in the Era of Antimicrobial Resistance: A Review', *Frontiers in Microbiology*, 10, p. 539. doi:10.3389/fmicb.2019.00539.

Mumper, R.J. *et al.* (1994) 'Calcium-alginate beads for the oral delivery of transforming growth factor-β1 (TGF-β1): stabilization of TGF-β1 by the addition of polyacrylic acid within acid-treated beads', *Journal of Controlled Release*, 30(3), pp. 241–251. doi:10.1016/0168-3659(94)90030-2.

Narayanan, S. *et al.* (2014) 'Mechanism of Escherichia coli Resistance to Pyrrhocoricin', *Antimicrobial Agents and Chemotherapy*, 58(5), pp. 2754–2762. doi:10.1128/AAC.02565-13.

Pacor, S. *et al.* (2021) 'The proline-rich myticalins from Mytilus galloprovincialis display a membrane-permeabilizing antimicrobial mode of action', *Peptides*, 143, p. 170594. doi:10.1016/j.peptides.2021.170594.

Pant, J. *et al.* (2019) 'Antibacterial 3D bone scaffolds for tissue engineering application', *Journal of Biomedical Materials Research Part B: Applied Biomaterials*, 107(4), pp. 1068–1078. doi:10.1002/jbm.b.34199.

Paris, J.L. *et al.* (2015) 'Tuning dual-drug release from composite scaffolds for bone regeneration', *International Journal of Pharmaceutics*, 486(1–2), pp. 30–37. doi:10.1016/j.ijpharm.2015.03.048.

Parisi, L. *et al.* (2018) 'Tailoring the Interface of Biomaterials to Design Effective Scaffolds', *Journal of Functional Biomaterials*, 9(3), p. 50. doi:10.3390/jfb9030050.

Peña, J. *et al.* (2010) 'An alternative technique to shape scaffolds with hierarchical porosity at physiological temperature', *Acta Biomaterialia*, 6(4), pp. 1288–1296. doi:10.1016/j.actbio.2009.10.049.

Podda, E. *et al.* (2006) 'Dual mode of action of Bac7, a proline-rich antibacterial peptide', *Biochimica et Biophysica Acta (BBA) - General Subjects*, 1760(11), pp. 1732–1740. doi:10.1016/j.bbagen.2006.09.006.

Porrelli, D. *et al.* (2015) 'Alginate-Hydroxyapatite Bone Scaffolds with Isotropic or Anisotropic Pore Structure: Material Properties and Biological Behavior: Alginate-Hydroxyapatite Bone Scaffolds with Isotropic…', *Macromolecular Materials and Engineering*, 300(10), pp. 989–1000. doi:10.1002/mame.201500055.

Porrelli, D. *et al.* (2021) 'Alginate bone scaffolds coated with a bioactive lactose modified chitosan for human dental pulp stem cells proliferation and differentiation', *Carbohydrate Polymers*, 273, p. 118610. doi:10.1016/j.carbpol.2021.118610.

Qi, J. *et al.* (2021) 'Current Biomaterial-Based Bone Tissue Engineering and Translational Medicine', *International Journal of Molecular Sciences*, 22(19), p. 10233. doi:10.3390/ijms221910233.

Reichert, J.C. *et al.* (2009) 'The challenge of establishing preclinical models for segmental bone defect research', *Biomaterials*, 30(12), pp. 2149–2163. doi:10.1016/j.biomaterials.2008.12.050.

Rimondini, L. *et al.* (2005) 'In vivo experimental study on bone regeneration in critical bone defects using an injectable biodegradable PLA/PGA copolymer', *Oral Surgery, Oral Medicine, Oral Pathology, Oral Radiology, and Endodontology*, 99(2), pp. 148–154. doi:10.1016/j.tripleo.2004.05.010.

Riool, M. *et al.* (2017) 'Antimicrobial Peptides in Biomedical Device Manufacturing', *Frontiers in Chemistry*, 5, p. 63. doi:10.3389/fchem.2017.00063.

Roberts, T.T. and Rosenbaum, A.J. (2012) 'Bone grafts, bone substitutes and orthobiologics: The bridge between basic science and clinical advancements in fracture healing', *Organogenesis*, 8(4), pp. 114–124. doi:10.4161/org.23306.

Roddy, E. *et al.* (2018) 'Treatment of critical-sized bone defects: clinical and tissue engineering perspectives', *European Journal of Orthopaedic Surgery & Traumatology*, 28(3), pp. 351–362. doi:10.1007/s00590-017-2063-0.

Román, J. *et al.* (2011) 'Control of the pore architecture in three-dimensional hydroxyapatite-reinforced hydrogel scaffolds', *Science and Technology of Advanced Materials*, 12(4), p. 045003. doi:10.1088/1468-6996/12/4/045003.

Runti, G. *et al.* (2017) 'The Mechanism of Killing by the Proline-Rich Peptide Bac7(1–35) against Clinical Strains of Pseudomonas aeruginosa Differs from That against Other Gram-Negative Bacteria', *Antimicrobial Agents and Chemotherapy*, 61(4). doi:10.1128/AAC.01660-16.

Sánchez-Salcedo, S., Nieto, A. and Vallet-Regí, M. (2008) 'Hydroxyapatite/β-tricalcium phosphate/agarose macroporous scaffolds for bone tissue engineering', *Chemical Engineering Journal*, 137(1), pp. 62–71. doi:10.1016/j.cej.2007.09.011.

Scocchi, M., Tossi, A. and Gennaro, R. (2011) 'Proline-rich antimicrobial peptides: converging to a non-lytic mechanism of action', *Cellular and Molecular Life Sciences*, 68(13), pp. 2317–2330. doi:10.1007/s00018-011-0721-7.

Shachar, M. *et al.* (2011) 'The effect of immobilized RGD peptide in alginate scaffolds on cardiac tissue engineering', *Acta Biomaterialia*, 7(1), pp. 152–162. doi:10.1016/j.actbio.2010.07.034.

Sharma, C. *et al.* (2016) 'Fabrication and characterization of novel nano-biocomposite scaffold of chitosan–gelatin–alginate–hydroxyapatite for bone tissue engineering', *Materials Science and Engineering: C*, 64, pp. 416–427. doi:10.1016/j.msec.2016.03.060.

Shibuya, N. and Jupiter, D.C. (2015) 'Bone Graft Substitute', *Clinics in Podiatric Medicine and Surgery*, 32(1), pp. 21–34. doi:10.1016/j.cpm.2014.09.011.

Sohn, H.-S. and Oh, J.-K. (2019) 'Review of bone graft and bone substitutes with an emphasis on fracture surgeries', *Biomaterials Research*, 23(1), p. 9. doi:10.1186/s40824-019-0157-y.

Sola, R. *et al.* (2020) 'Characterization of Cetacean Proline-Rich Antimicrobial Peptides Displaying Activity against ESKAPE Pathogens', *International Journal of Molecular Sciences*, 21(19), p. 7367. doi:10.3390/ijms21197367.

Souza, P.R. *et al.* (2021) 'Polysaccharide-Based Materials Created by Physical Processes: From Preparation to Biomedical Applications', *Pharmaceutics*, 13(5), p. 621. doi:10.3390/pharmaceutics13050621.

Sukhodub, L.F. *et al.* (2018) 'Synthesis and characterization of hydroxyapatite-alginate nanostructured composites for the controlled drug release', *Materials Chemistry and Physics*, 217, pp. 228–234. doi:10.1016/j.matchemphys.2018.06.071.

Sun, J. and Tan, H. (2013) 'Alginate-Based Biomaterials for Regenerative Medicine Applications', *Materials*, 6(4), pp. 1285–1309. doi:10.3390/ma6041285.

Toppazzini, M. *et al.* (2011) 'Can the interaction between the antimicrobial peptide LL-37 and alginate be exploited for the formulation of new biomaterials with antimicrobial properties?', *Carbohydrate Polymers*, 83(2), pp. 578–585. doi:10.1016/j.carbpol.2010.08.020.

Trampuz, A. and Zimmerli, W. (2006) 'Antimicrobial Agents in Orthopaedic Surgery: Prophylaxis and Treatment', *Drugs*, 66(8), pp. 1089–1105. doi:10.2165/00003495-200666080-00005.

Turco, G. *et al.* (2009) 'Alginate/Hydroxyapatite Biocomposite For Bone Ingrowth: A Trabecular Structure With High And Isotropic Connectivity', *Biomacromolecules*, 10(6), pp. 1575–1583. doi:10.1021/bm900154b.

Venkatesan, J. *et al.* (2015) 'Alginate composites for bone tissue engineering: A review', *International Journal of Biological Macromolecules*, 72, pp. 269–281. doi:10.1016/j.ijbiomac.2014.07.008.

Ventola, C.L. (2015 a) 'The Antibiotic Resistance Crisis', *Pharmacy and Therapeutics* p. 7.

Ventola, C.L. (2015 b) 'The Antibiotic Resistance Crisis', *Pharmacy and Therapeutics* p. 9.

Wang, W. and Yeung, K.W.K. (2017) 'Bone grafts and biomaterials substitutes for bone defect repair: A review', *Bioactive Materials*, 2(4), pp. 224–247. doi:10.1016/j.bioactmat.2017.05.007.

Williams, D.F. (2008) 'On the mechanisms of biocompatibility', *Biomaterials*, 29(20), pp. 2941–2953. doi:10.1016/j.biomaterials.2008.04.023.

Winkler, T. *et al.* (2018) 'A review of biomaterials in bone defect healing, remaining shortcomings and future opportunities for bone tissue engineering: The unsolved challenge', *Bone & Joint Research*, 7(3), pp. 232–243. doi:10.1302/2046-3758.73.BJR-2017-0270.R1.

Witzler, M. *et al.* (2019) 'Non-Cytotoxic Agarose/Hydroxyapatite Composite Scaffolds for Drug Release', *International Journal of Molecular Sciences*, 20(14), p. 3565. doi:10.3390/ijms20143565.

Xhindoli, D. *et al.* (2016) 'The human cathelicidin LL-37 — A pore-forming antibacterial peptide and host-cell modulator', *Biochimica et Biophysica Acta (BBA) - Biomembranes*, 1858(3), pp. 546–566. doi:10.1016/j.bbamem.2015.11.003.

Yehouenou, C.L. *et al.* (2020) 'Antimicrobial resistance in hospitalized surgical patients: a silently emerging public health concern in Benin', *Annals of Clinical Microbiology and Antimicrobials*, 19(1), p. 54. doi:10.1186/s12941-020-00398-4.

Zhang, R. and Ma, P.X. (1999) 'Poly(?-hydroxyl acids)/hydroxyapatite porous composites for bone-tissue engineering. I. Preparation and morphology', *Journal of Biomedical Materials Research*, 44(4), pp. 446–455. doi:10.1002/(SICI)1097-4636(19990315)44:4<446::AID-JBM11>3.0.CO;2-F.

Zimmerli, W. and Sendi, P. (2017) ‘Orthopaedic biofilm infections’, *APMIS*, 125(4), pp. 353–364. doi:10.1111/apm.12687.

APPENDIX - COLLATERALS ACTITIVIES AND PAPERS PUBLISHED DURING THE Ph.D.

Doti N, Mardirossian M, Sandomenico A, Ruvo M, Caporale A. (2021) Recent applications of retro-inverso peptides. *Int J Mol Sci.*

Natural and de novo designed peptides are gaining an ever-growing interest as drugs against several diseases. Their use is however limited by the intrinsic low bioavailability and poor stability. To overcome these issues retro-inverso analogues have been investigated for decades as more stable surrogates of peptides composed of natural amino acids. Retro-inverso peptides possess reversed sequences and chirality compared to the parent molecules maintaining at the same time an identical array of side chains and in some cases similar structure. The inverted chirality renders them less prone to degradation by endogenous proteases conferring enhanced half-lives and an increased potential as new drugs. However, given their general incapability to adopt the 3D structure of the parent peptides their application should be careful evaluated and investigated case by case. Here, we review the application of retro-inverso peptides in anticancer therapies, in immunology, in neurodegenerative diseases, and as antimicrobials, analyzing pros and cons of this interesting subclass of molecules.

Armas F, Di Stasi A, Mardirossian M, Romani A, Benincasa M, Scocchi M. (2021) Effects of Lipidation on a Proline-Rich Antibacterial Peptide. *Int J Mol Sci.*

The emergence of multidrug-resistant bacteria is a worldwide health problem. Antimicrobial peptides have been recognized as potential alternatives to conventional antibiotics, but still require optimization. The proline-rich antimicrobial peptide Bac7(1-16) is active against only a limited number of Gram-negative bacteria. It kills bacteria by inhibiting protein synthesis after its internalization, which is mainly supported by the bacterial transporter SbmA. In this study, we tested two different lipidated forms of Bac7(1-16) with the aim of extending its activity against those bacterial species that lack SbmA. We linked a C12-alkyl chain or an ultrashort cationic lipopeptide Lp-I to the C-terminus of Bac7(1-16). Both the lipidated Bac-C12 and Bac-Lp-I forms acquired activity at low micromolar MIC values against several Gram-positive and Gram-negative bacteria. Moreover, unlike Bac7(1-16), Bac-C12, and Bac-Lp-I did not select resistant mutants in E. coli after 14 times of exposure to sub-MIC concentrations of the respective peptide. We demonstrated that the extended spectrum of activity and absence of de novo resistance are likely related to the acquired capability of the peptides to permeabilize cell membranes. These results indicate that C-terminal lipidation of a short proline-rich peptide profoundly alters its function and mode of action and provides useful insights into the design of novel broad-spectrum antibacterial agents.

Pacor S, Benincasa M, Musso MV, Krce L, Aviani I, Pallavicini A, Scocchi M, Gerdol M, Mardirossian M. (2021) The proline-rich myticalins from Mytilus galloprovincialis display a membrane-permeabilizing antimicrobial mode of action. *Peptides.*

Bivalve mollusks are continuously exposed to potentially pathogenic microorganisms living in the marine environment. Not surprisingly, these filter-feeders developed a robust innate immunity to protect themselves, which includes a broad panel of antimicrobial peptides. Among these, myticalins represent a recently discovered family of linear cationic peptides expressed in the gills of Mytilus galloprovincialis. Even though myticalins and insect and mammalian proline-rich antimicrobial peptides (PrAMPs) share a similar amino acid composition, we here show that none of the tested mussel peptides use a non-lytic mode of action relying on the bacterial transporter SbmA. On the other hand, all the tested myticalins perturbed and permeabilized the membranes of E. coli BW25113, as shown by flow-cytometry and atomic force microscopy. Circular dichroism spectra revealed that most myticalins did not adopt recognizable secondary structures in the presence of amphipathic environments, such as biological membranes. To explore possible uses of myticalins for

biotech, we assessed their biocompatibility with a human cell line. Non-negligible cytotoxic effects displayed by myticalins indicate that their optimization would be required before their further use as lead compounds in the development of new antibiotics.

Porrelli D, Mardirossian M, Crapisi N, Urbam M, Ulian NA, Bevilacqua L, Turco G, Maglione M. (2021) Polyetheretherketone and titanium surface treatments to modify roughness and wettability – Improvement of bioactivity and antibacterial properties. ***J of Mat Sci Tech.***

Among the materials available for implant production, titanium is the most used while polyetheretherketone (PEEK) is emerging thanks to its stability and to the mechanical properties similar to the ones of the bone tissue. Material surface properties like roughness and wettability play a paramount role in cell adhesion, cell proliferation, osteointegration and implant stability. Moreover, the bacterial adhesion to the biomaterial and the biofilm formation depend on surface smoothness and hydrophobicity. In this work, two different treatments, sandblasting and air plasma, were used to increase respectively roughness and wettability of two materials: titanium and PEEK. Their effects were analyzed with profilometry and contact angle measurements. The biological properties of the material surfaces were also investigated in terms of cell adhesion and proliferation of NIH-3T3 cells, MG63 cells and human Dental Pulp Stem Cells. Moreover, the ability of Staphylococcus aureus to adhere and form a viable biofilm on the samples was evaluated. The biological properties of both treatments and both materials were compared with samples of Synthegra® titanium, which underwent laser ablation to obtain a porous micropatterning, characterized by a smooth surface to discourage bacterial adhesion. All cell types used were able to adhere and proliferate on samples of the tested materials. Cell adhesion was higher on sandblasted PEEK samples for both MG63 and NIH-3T3 cell lines, on the contrary, the highest proliferation rate was observed on sandblasted titanium and was only slightly dependent on wettability; hDPSCs were able to proliferate similarly on sandblasted samples of both tested materials. The highest osteoblast differentiation was observed on laser micropatterned titanium samples, but similar effects, even if limited, were also observed on both sandblasted materials and air plasma treated titanium. The lowest bacterial adhesion and biofilm formation was observed on micropatterned titanium samples whereas, the highest biofilm formation was detected on sandblasted PEEK samples, and in particular on samples not treated with air-plasma, which displayed the highest hydrophobicity. The results of this work showed that all the tested materials were able to sustain osteoblast adhesion and promote cell proliferation; moreover, this work highlights the feasible PEEK treatments which allow to obtain surface properties similar to those of titanium. The results here reported, clearly show that cell behavior depends on a complex combination of surface properties like wettability and roughness and material nature, and while a rough surface is optimal for cell adhesion, a smooth and less hydrophilic surface is the best choice to limit bacterial adhesion and biofilm formation.

Porrelli D, Mardirossian M, Musciacchio L, Pacor M, Berton F, Crosera M, Turco G. (2021) Antibacterial electrospun polycaprolactone membranes coated with polysaccharides and silver nanoparticles for guided bone and tissue regeneration. ***ACS Appl Mater Interfaces.***

Electrospun polycaprolactone (PCL) membranes have been widely explored in the literature as a solution for several applications in tissue engineering and regenerative medicine. PCL hydrophobicity and its lack of bioactivity drastically limit its use in the medical field. To overcome these drawbacks, many promising strategies have been developed and proposed in the literature. In order to increase the bioactivity of electrospun PCL membranes designed for guided bone and tissue regeneration purposes, in the present work, the membranes were functionalized with a coating of bioactive lactose-modified chitosan (CTL). Since CTL can be used for the synthesis and stabilization of silver nanoparticles, a coating of this compound was employed here to provide antibacterial properties to the membranes. Scanning electron microscopy imaging revealed that the electrospinning process adopted here allowed us to obtain membranes with homogeneous fibers and without defects. Also, PCL membranes retained their mechanical properties after several weeks of aging in

simulated body fluid, representing a valid support for cell growth and tissue development. CTL adsorption on membranes was investigated by fluorescence microscopy using fluorescein-labeled CTL, resulting in a homogeneous and slow release over time. Inductively coupled plasma–mass spectrometry was used to analyze the release of silver, which was shown to be stably bonded to the CTL coating and to be slowly released over time. The CTL coating improved MG63 osteoblast adhesion and proliferation on membranes. On the other hand, the presence of silver nanoparticles discouraged biofilm formation by Pseudomonas aeruginosa and Staphylococcus aureus without being cytotoxic. Overall, the stability and the biological and antibacterial properties make these membranes a valid and versatile material for applications in guided tissue regeneration and in other biomedical fields like wound healing.

Rupel K, Zupin L, Brich S, Mardirossian M, Ottaviani G, Gobbo M, Di Lenarda R, Pricl S, Crovella S, Zacchigna S, Biasotto M. (2021) Antimicrobial activity of amphiphilic nanomicelles loaded with curcumin against *Pseudomonas aeruginosa* alone and activated by blue laser light. *J Biophotonics*.

The aim of this work was to assess the antimicrobial efficacy on Pseudomonas aeruginosa of nanomicelles loaded with curcumin (CUR) alone and activated by blue laser light in an antimicrobial photodynamic therapy (APDT) approach. First, free CUR in liquid suspension and loaded in three amphiphilic nanomicelles (CUR-DAPMA, CUR-SPD and CUR-SPM) were tested both on bacteria and keratinocytes. While free CUR exerted limited efficacy showing moderate cytotoxicity, a strong inhibition of bacterial growth was obtained using all three nanosystems without toxicity on eukaryotic cells. CUR-SPM emerged as the most effective, and was therefore employed in APDT experiments. Among the three sublethal blue laser (λ 445 nm) protocols tested, the ones characterized by a fluence of 18 and 30 J/cm2 further decreased the antimicrobial concentration to 50 nM. The combination of blue laser APDT with CUR-SPM nanomicelles results in an effective synergistic activity that represents a promising novel therapeutic approach on resistant species.

Sola R, Mardirossian M, Beckert B, De Luna LS, Prickett D, Tossi A, Wilson DN, Scocchi M. (2020) Characterization of cetacean proline-rich antimicrobial peptides displaying activity against eskape pathogens. *Int J Mol Sci.*

Proline-rich antimicrobial peptides (PrAMPs) may be a valuable weapon against multi-drug resistant pathogens, combining potent antimicrobial activity with low cytotoxicity. We have identified novel PrAMPs from five cetacean species (cePrAMPs), and characterized their potency, mechanism of action and in vitro cytotoxicity. Despite the homology between the N-terminal of cePrAMPs and the bovine PrAMP Bac7, some differences emerged in their sequence, activity spectrum and mode of action. CePrAMPs with the highest similarity with the Bac7(1-35) fragment inhibited bacterial protein synthesis without membrane permeabilization, while a second subgroup of cePrAMPs was more membrane-active but less efficient at inhibiting bacterial translation. Such differences may be ascribable to differences in presence and positioning of Trp residues and of a conserved motif seemingly required for translation inhibition. Unlike Bac7(1-35), which requires the peptide transporter SbmA for its uptake, the activity of cePrAMPs was mostly independent of SbmA, regardless of their mechanism of action. Two peptides displayed a promisingly broad spectrum of activity, with minimal inhibiting concentration MIC $\leq$ 4 μM against several bacteria of the ESKAPE group, including Pseudomonas aeruginosa and Enterococcus faecium. Our approach has led us to discover several new peptides; correlating their sequences and mechanism of action will provide useful insights for designing optimized future peptide-based antibiotics.

Mardirossian M, Sola R, Beckert B, Valencic E, Collis DWP, Borišek J, Armas F, Di Stasi A, Buchmann J, Syroegin EA, Polikanov YS, Magistrato A, Hilpert K, Wilson DN, Scocchi M. (2020) Peptide Inhibitors of Bacterial Protein Synthesis with Broad Spectrum and SbmA-Independent Bactericidal Activity against Clinical Pathogens. *J Med Chem.*

Proline-rich antimicrobial peptides (PrAMPs) are promising lead compounds for developing new antimicrobials; however, their narrow spectrum of action is limiting. PrAMPs kill bacteria binding to their ribosomes and inhibiting protein synthesis. In this study, 133 derivatives of the PrAMP Bac7(1–16) were synthesized to identify the crucial residues for ribosome inactivation and antimicrobial activity. Then, five new Bac7(1–16) derivatives were conceived and characterized by antibacterial and membrane permeabilization assays, X-ray crystallography, and molecular dynamics simulations. Some derivatives displayed broad spectrum activity, encompassing Escherichia coli, Klebsiella pneumoniae, Acinetobacter baumanii, Pseudomonas aeruginosa, and Staphylococcus aureus. Two peptides out of five acquired a weak membrane-perturbing activity while maintaining the ability to inhibit protein synthesis. These derivatives became independent of the SbmA transporter, commonly used by native PrAMPs, suggesting that they obtained a novel route to enter bacterial cells. PrAMP-derived compounds could become new-generation antimicrobials to combat antibiotic-resistant pathogens.

Degasperi M, Agostinis C, Mardirossian M, Maschio M, Taddio A, Bulla R, Scocchi M. (2020) The anti-pseudomonal peptide d-bmap18 is active in cystic fibrosis sputum and displays anti-inflammatory in vitro activity. *Microorganisms.*

Most Cystic Fibrosis (CF) patients succumb to airway inflammation and pulmonary infections due to Pseudomonas aeruginosa. D-BMAP18, a membrane-permeabilizing antimicrobial peptide composed of D-amino acids, was evaluated as a possible antibacterial aimed to address this issue. The antipseudomonal activity of D-BMAP18 was tested in a pathophysiological context. The peptide displayed activity against CF isolates of Pseudomonas aeruginosa in the presence of CF sputum when combined with sodium chloride and DNase I. In combination with DNase I, D-BMAP18 discouraged the deposition of new biofilm and eradicated preformed biofilms of some P. aeruginosa strains. In addition, D-BMAP18 down regulated the production of TNF-α, IL1-β, and TGF-β in LPS-stimulated or IFN-γ macrophages derived from THP-1 cells indicating an anti-inflammatory activity. The biocompatibility of D-BMAP18 was assessed using four different cell lines, showing that residual cell-specific cytotoxicity at bactericidal concentrations could be abolished by the presence of CF sputum. Overall, this study suggests that D-BMAP18 may be an interesting molecule as a starting point to develop a novel therapeutic agent to simultaneously contrast lung infections and inflammation in CF patients.

Berton F, Porrelli D, Turco G, Mardirossian M, Nicolin V, Rizzo R, Stacchi C, Di Lenarda R. (2019) L-PRF enrichment with nanohydroxiapatite: an in vitro proof of concept study. *Global J Oral Sci.*

Nowadays platelet concentrates (PCs) show interesting potential in oral surgery for soft tissue healing promotion. However, inductive properties for bone formation remains still controversial. Recently, numerous studies explored the merging of two different tissue healing inducing agents: PCs with osteoinducing agents or scaffolds or antiresorptive drugs. Research trend looks towards the amelioration of the inductive properties of PCs, mainly towards bone regeneration. This paper aims to evaluate i) the durability of the pristine L-PRF membranes in dissolution assay; ii) the opportunity of coupling the obtained membranes with an osteoconductive molecule, such as nanohydroxyapatites (nHAp). Thus, the durability of pristine membrane in SBF was tested. At each time point, one sample was analyzed with SEM; image processing revealed an average fiber diameter of 0.103 ± 0.05μm without any statistically significant differences during time. Degradation assay showed a two-folds increase of the weight related to the SBF absorption in the first 2 days. From the third day a constant degradation was observed. In the time frame of this experiment, the dimensional stability

of the fibrin structure up to day 7 suggested that PRF membranes may also be used uncovered in the oral cavity. Subsequently, the effects of the nHAp addition during the forming process of PRF (thus during centrifugation) were investigated.

Mardirossian M, Sola R, Beckert B, Collis DWP, Di Stasi A, Armas F, Hilpert K, Wilson DN, Scocchi M. (2019) Proline-rich peptides with improved antimicrobial activity against *E. coli, K. pneumoniae, and A. baumannii*. *Chem Med Chem.*

Proline-rich antimicrobial peptides (PrAMPs) are promising agents to combat multi-drug resistant pathogens due to a high antimicrobial activity, yet low cytotoxicity. A library of derivatives of the PrAMP Bac5(1-17) was synthesized and screened to identify which residues are relevant for its activity. In this way, we discovered that two central motifs -PIRXP- cannot be modified, while residues at N- and C- termini tolerated some variations. We found five Bac5(1-17) derivatives bearing 1-5 substitutions, with an increased number of arginine and/or tryptophan residues, exhibiting improved antimicrobial activity and broader spectrum of activity while retaining low cytotoxicity toward eukaryotic cells. Transcription/translation and bacterial membrane permeabilization assays showed that these new derivatives still retained the ability to strongly inhibit bacterial protein synthesis, but also acquired permeabilizing activity to different degrees. These new Bac5(1-17) derivatives therefore show a dual mode of action which could hinder the selection of bacterial resistance against these molecules.